https://doi.org/10.5194/egusphere-2025-5627
Preprint. Discussion started: 5 January 2026

Ground-based total ozone column measurements in the Huggins and Chappuis bands using Direct-Sun DOAS observations

Dimitris Karagkiozidis[1], Alkiviadis Bais[1], Katerina Garane[1], Michel Van Roozendael[2], Dimitris Nikolis[1], Manuel Roca[3] and Dimitris Balis[1]

[1]Laboratory of Atmospheric Physics, Aristotle University of Thessaloniki, 54124 Thessaloniki, Greece
[2]Royal Belgian Institute for Space Aeronomy (BIRA-IASB), 1180 Brussels, Belgium
[3]LuftBlick, Fritz-Konzert-Straße 4, 6020 Innsbruck, Austria

Correspondence to: Dimitris Karagkiozidis (dkaragki@auth.gr)

Abstract. Accurate routine monitoring of the Total Ozone Column (TOC) is essential for understanding ozone temporal variability, assessing long-term trends and supporting satellite validation. In this work, we present TOC retrievals in both ultraviolet (Huggins bands) and visible (Chappuis bands) spectral regions using direct-sun Differential Optical Absorption Spectroscopy (DS-DOAS). We use the Delta UV–VIS DOAS system, recently designed and operated at the Laboratory of Atmospheric Physics in Thessaloniki, Greece. A dedicated retrieval algorithm was developed that includes the calibration of a measured reference DS spectrum using the Langley plot and Bootstrap Estimation approaches. The analysis suggests that TOCs derived from the visible channel for the first time in Thessaloniki are highly consistent with those from the ultraviolet channel, with a median difference of –0.44% and Pearson's correlation coefficient R=0.97. The Delta TOC retrievals were compared with two collocated instruments, Brewer and Pandora, yielding very good agreement in both spectral regions (R>0.98), with median biases –0.18% and –0.63% for the VIS and 0.08% and –0.32% for the UV channel compared to the Brewer and Pandora, respectively. The seasonal and diurnal variabilities of total ozone were captured consistently from all three instruments, confirming the robustness of the retrievals. Enhanced aerosol loads, such as those observed during an extreme wildfire event, introduced significant deviations in the VIS TOC comparisons with the reference instruments, while the comparisons in the UV remained largely unaffected. The findings of this study confirm the capability of Delta to provide accurate and consistent TOC retrievals in both UV and VIS spectral bands. The successful exploitation of the Chappuis bands extends the applicability of DS-DOAS to conditions where UV sensitivity is limited, such as at high solar zenith angles, thereby extending the continuity of ozone monitoring from ground-based systems and providing a complementary approach to traditional UV-based TOC retrievals.

1 Introduction

Ozone (O_3), one of the most important and well-known trace gases in the atmosphere (WMO, 2022), plays a key role in atmospheric chemistry, radiative forcing, air-quality and climate change (Crutzen, 1979). Approximately 90% of the Total Ozone Column (TOC) resides in the stratosphere, with highest concentrations at altitudes between 20 and 30 km (Seinfeld and Pandis, 2016; Langematz, 2019). By absorbing nearly all harmful ultraviolet (UV) solar radiation at wavelengths below 290

https://doi.org/10.5194/egusphere-2025-5627
Preprint. Discussion started: 5 January 2026

nm and also a large fraction of the short-wave UV-B solar radiation, between 290 and 315 nm, stratospheric O_3 has a strong impact on the global radiative forcing and is essential for the biosphere, protecting humans and natural ecosystems. In the troposphere, ozone plays a key role in the oxidizing capacity of the atmosphere (Lelieveld et al., 2016) and acts as a greenhouse gas contributing to radiative forcing. Near the surface it is widely recognized as a secondary pollutant, produced by photochemical reactions of nitrogen oxides (NO_X) and Volatile Organic Compounds (VOCs), having a strong impact on human health, vegetation and ecosystems (Fowler et al., 2009; Monks et al., 2015; Young et al., 2018).

Routine measurements of TOC began in the 1920s with the use of the Dobson spectrophotometer (Dobson, 1931), later superseded by the automated Brewer spectrophotometer, developed in the late 1970s (Brewer, 1973; Kerr et al., 1981, 1988). Both systems have been extensively used over the past decades for ozone monitoring. Especially after the discovery of the so-called "Antarctic ozone hole" in the mid-1980s (Farman et al., 1985; Chubachi, 1985), they played a critical role in assessing ozone trends and their links on climate change. Numerous studies have been conducted on the variability of stratospheric ozone and its long-term trends, on a global scale, based on both ground-based data measured by Dobson and Brewer instruments, as well as satellite observations (e.g., Harris et al., 1997; Zerefos et al., 2001; Fioletov et al., 2002; Ziemke et al., 2005). With the successful implementation of the Montreal Protocol (Mäder et al., 2010), the abundance of ozone-depleting substances (ODSs) in the stratosphere has been reduced and several studies have indicated a gradual recovery of TOC levels in recent years (Solomon et al., 2016; Kuttippurath and Nair, 2017; Pazmiño et al., 2018; Weber et al., 2022). Nevertheless, maintaining high-quality ground-based TOC observations remains of high importance. Despite their historical significance, Dobson and Brewer instruments are no longer produced and the required technical support for uninterrupted operation is very limited. The number of stations contributing TOC data to the global observing network is decreasing, while those that remain active and operational require regular high-cost calibration and maintenance procedures. To ensure the continuity of accurate TOC measurements and to further expand our knowledge on the interactions of ozone and climate change, gradual transitioning to alternative TOC measurement techniques is of high research and environmental significance.

Passive Differential Optical Absorption Spectroscopy (DOAS) is a well-established and widely used remote sensing method that has been applied since the 1970s for the detection of numerous trace gases, including O_3, in the atmosphere, with characteristic narrow-band absorption structures in the UV and visible (VIS) spectral range (Platt and Stutz, 2008). Over time, DOAS has been adapted for multiple applications using different viewing geometries, each being sensitive to different altitudes within the atmosphere, depending on the target species. The principal idea of all passive DOAS applications is the same: in a first step, the trace gas Slant Column Density (SCD) is retrieved from spectral analysis, which is then converted to a Vertical Column Density (VCD) by division with an appropriate Air-Mass-Factor (AMF) (Noxon, 1979; Solomon et al., 1987a). Zenith-Sky (ZS) DOAS measurements were one of the earliest passive DOAS implementations and have been used in various studies about stratospheric nitrogen dioxide (NO_2) (Brewer, 1973; Noxon, 1975), as well as O_3 and chlorine oxide (OClO) (e.g., Mount et al., 1987; Solomon et al., 1987b, 1988). ZS-DOAS instruments, such as the Système d'Analyse par Observation Zénithale (SAOZ; Pommereau and Goutail, 1988), most of which are part of the Network for Detection of Atmospheric Composition Change (NDACC), are sensitive to stratospheric absorbers. They rely on scattered radiation spectra measured at

https://doi.org/10.5194/egusphere-2025-5627
Preprint. Discussion started: 5 January 2026

the zenith during twilight, at high Solar Zenith Angles (SZAs), thus providing measurements of O_3 twice a day, i.e., at sunrise and at sunset (Van Roozendael et al., 1998; Hendrick et al., 2011). The AMF for ZS-DOAS depends on several atmospheric parameters, such as the O_3 vertical profile, surface albedo, as well as temperature and pressure profiles (Cede et al., 2006; Hendrick et al., 2011) and its calculation is based on Radiative Transfer Model (RTM) simulations. Direct-Sun (DS) DOAS is another application of DOAS that is equally sensitive to stratospheric and tropospheric absorbers for SZAs < 80°. It yields information about the total VCD, i.e., from ground level up to the top of the atmosphere and unlike ZS-DOAS, it allows for potential investigation of diurnal cycles. The AMF for direct sun observations can be easily approximated with a geometric approach, however, compared to other viewing geometries, e.g., such as those employed in Multi-AXis Differential Optical Absorption Spectroscopy (MAX-DOAS) measurements (Hönninger et al., 2004), the photon path lengths are relatively small leading to weaker signals, thus systems with high Signal to Noise Ratio (SNR) are usually required. TOC measurements employing the DS-DOAS technique have been used in various studies (e.g., Tzortziou et al., 2012, 2015; Herman et al., 2015; Kim et al., 2017; Gkertsi et al., 2018). In recent years, Pandora systems have been developed to provide standardized DS-DOAS measurements of ozone and other trace gases. These instruments form the Pandonia Global Network (PGN), which delivers quality-assured, near-real-time data products and plays an increasingly important role in long-term monitoring and satellite validation.

TOC retrievals from direct sun observations are traditionally conducted in the UV, typically within the wavelength range of 300 – 360 nm, where ozone exhibits distinct narrow-band absorption features, known as Huggins bands. However, ozone also shows weaker, but still significant structures in the visible and near-infrared (NIR) regions between 400 and 650 nm, referred to as Chappuis absorption bands. Using measurements in this spectral region has several benefits. Retrievals in the visible range are less sensitive to stray-light interference, which often limits the accuracy of UV-based measurements, especially at high SZAs. Furthermore, many commercially available and research-grade spectrometers either lack sufficient sensitivity in the UV or are designed primarily for the visible region and therefore, employing measurements in the Chappuis bands broadens the range of instruments that can be used for TOC monitoring. In addition, retrievals in the visible range provide an advantage for high-latitude and wintertime observations, where solar UV radiation is relatively weak and often limits the applicability of measurements in the Huggins bands. Under such conditions, solar radiation in the visible range is more intense, allowing the Chappuis bands to be exploited for TOC retrievals, thereby supporting the continuity of ozone monitoring, which is essential for maintaining consistent long-term records and for providing reliable reference data for satellite validation in polar and subpolar regions. To our knowledge, direct-sun observations in the Chappuis bands have not been previously used for TOC retrievals, and this study introduces such an application for the first time.

The aim of this work is to retrieve TOC both in the UV and VIS regions, by applying a DOAS-based algorithm to direct sun spectra recorded by the Delta UV-VIS system, operating at the Laboratory of Atmospheric Physics (LAP), in Thessaloniki, Greece. By conducting an intercomparison study with collocated Brewer and Pandora TOC measurements, we aim to establish linkages among these independent sources of information on ozone. Such linkages will facilitate their synergistic use in future monitoring and research activities. Furthermore, they will strengthen the role of ground-based observations in supporting

https://doi.org/10.5194/egusphere-2025-5627
Preprint. Discussion started: 5 January 2026

satellite validation and in assessing regional ozone variability. Finally, the intercomparison provides a cross-checking framework that ensures internal consistency across the instruments, which is crucial for sustained ozone monitoring.

This article is structured as follows: In Sect. 2, a description is given for the instruments and datasets utilized in this study. In Sect. 3, the DOAS-based TOC retrieval methodology is presented along with the required calibration procedures. In Sect. 4, the intercomparison results with the Brewer and the Pandora are discussed, and in Sect. 5 the main conclusions of this study are summarized.

2 Instrumentation and data

2.1 The measurement site

Thessaloniki is the second-largest city in Greece, located in the northern part of the country with a coastal orientation facing the Aegean Sea, which is a part of the larger Mediterranean region. The measurement site is located in the city centre, on the rooftop of the School of Physics, at the Laboratory of Atmospheric Physics (40.633°N, 22.956°E, 60 m a.s.l) of the Aristotle University of Thessaloniki (LAP.AUTH; https://lapweb.physics.auth.gr/en/home-english/, last access: 8 November 2025). Thessaloniki holds historical significance in the field of ground-based TOC measurements and hosts a range of remote-sensing instruments designed for this purpose. In the 1980s, when the decline of stratospheric ozone levels was of high research and environmental importance, LAP.AUTH was equipped with the first commercially available single-monochromator Brewer with serial number 005 (hereafter BR005). It was installed in 1982, providing the capability to monitor for the first time TOC in Thessaloniki and also investigate its effect on solar UV irradiance at ground level. BR005 is still operational and regularly calibrated. TOC measurements over Thessaloniki are also performed since 2015 by a miniature spectrophotometer (Phaethon) by applying the DOAS technique on direct sun spectra (Gkertsi et al., 2018). Since June 2022, LAP.AUTH is equipped with a new research-grade spectrometer system (namely Delta), which represents a significant enhancement of the existing instrumentation as it is designed to provide higher quality spectral measurements and is characterized by increased accuracy and sensitivity, with the capability to apply DS-DOAS and to retrieve TOC. In late 2022, TOC measurements over Thessaloniki have further been supported through the installation of a Pandora 2S instrument that is part of PGN (https://www.pandonia-global-network.org/, last access: 8 November 2025), and provides columnar measurements of O_3 among other species, which are near-real-time, centrally processed, quality assured and distributed by PGN. The measurement site of LAP.AUTH along with the instrumentation utilized under the scope of this study are presented in Figure 1.

https://doi.org/10.5194/egusphere-2025-5627
Preprint. Discussion started: 5 January 2026

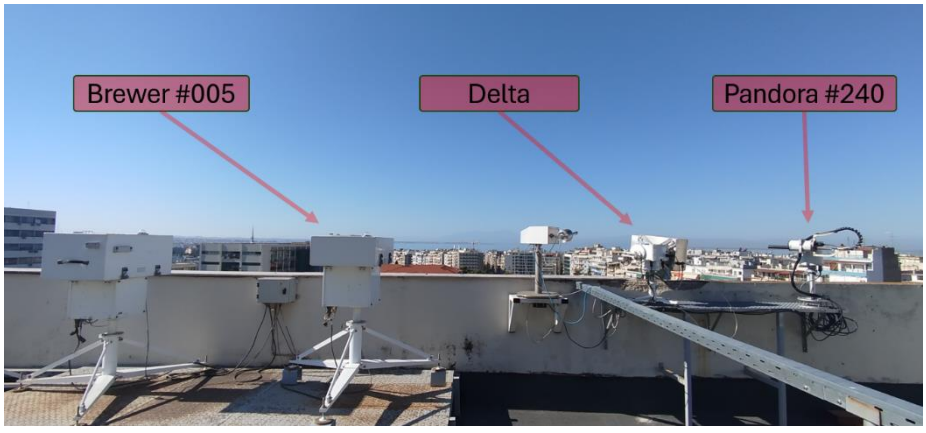

Figure 1: The measurement site of LAP.AUTH and the three collocated ground-based instruments used in this study: Brewer spectrophotometer #005 (left), Delta UV–VIS DOAS system (centre), and Pandora #240 (right).

2.2 The Delta system

Delta is a scientific-grade instrument developed in collaboration with the Royal Belgian Institute for Space Aeronomy (BIRA-IASB) in the framework of the PANhellenic infrastructure for Atmospheric Composition and Climate Change (PANACEA; https://panacea-ri.gr/?lang=en, last access: 8 November 2025) project. The system consists of two main parts: an optical head, which is located outdoors, mounted on a dual-axis sun tracker, and a single-channel acquisition unit, located inside the building, comprising a detector mounted on a spectrograph and a computer used for instrument control with a home-made software, data acquisition and data storage (Karagkiozidis, 2023). Light is collected by the optical head via a planoconvex lens, installed in its front part, and it is guided to the entrance slit of the spectrograph through a fiber bundle of rectangular ending. The spectrograph is a commercial Kymera 193i unit by Andor Oxford Instruments, which includes a grating of 600 grooves/mm, allowing for a wavelength coverage of ~ 230 nm. It is placed inside a thermo-regulated box, whose temperature is maintained constant at +20°C. The instrument's slit function was measured using mercury discharge lamp spectral lines and it was found to approximately correspond to a Gaussian with Full Width at Half Maximum (FWHM) of ~ 0.85 nm. Such lamp spectra are also used for accurate wavelength calibration. The spectral range of the spectrograph was set to 305 – 523 nm so that multiple trace gases can be detected using DOAS in the UV and visible regions (Platt and Stutz, 2008). The detector is a low-noise PIXIS 2KBUV back illuminated and UV enhanced charge-coupled device (CCD) of 2048×512 pixels by Princeton Instruments, which is thermo-electrically cooled to –50°C by means of a Peltier system, thereby suppressing generation of dark current. Depending on the measurement type, and to avoid saturation of the measured spectra, the light intensity can be attenuated by neutral-density optical filters, transmission diffuser plates and cut-off filters, one by one or in various combinations, which are placed on six positions of a filter-wheel, located inside the optical head. The optical head includes also a commercial dual-axis inclinometer by Jewell Instruments, used to ensure a precise levelling of the instrument and proper orientation of the optical head. The system was originally designed to collect scattered solar radiation at different elevation angles, required for MAX-DOAS measurements (Hönninger et al., 2004) for the retrieval of tropospheric aerosol (trace gas)

https://doi.org/10.5194/egusphere-2025-5627
Preprint. Discussion started: 5 January 2026

extinction (concentration) vertical profiles and integrated columns. However, the EKO STR-22G sun tracker allows orientation of the optical head at any given azimuth (0° – 360°) and elevation (0° – 90°) viewing direction, with a pointing resolution of less than 0.01°, thus providing also accurate direct sun capability. The first scientific application of the recently developed Delta system at LAP.AUTH has been the retrieval of total NO_2 vertical columns using the DS-DOAS technique (Nikolis et al., 2025), confirming its suitability for direct-sun trace gas observations. Simultaneous calibration of the azimuth and elevation angles is performed by regular sun scans, i.e., by sighting of the sun disk, an approach that was found to provide low systematic uncertainties of ±0.05° (Donner et al., 2020).

Since the beginning of its operation in 2022, the measurement schedule of Delta includes elevation scans at two azimuth directions, followed by a direct sun measurement. The total integration time of each elevation scan is ~ 15 min, hence direct sun observations are performed approximately every half an hour. Dark spectra are measured at nighttime (at SZAs higher than 105°) for 30 min and for all exposure times of the detector used during the daily cycles, which are then subtracted from the measured solar spectra, prior to the DOAS analysis. During the first year of operation in direct sun mode (until June 2023), the light throughput in the spectrograph was very high, as a result of inadequate attenuation of light intensity (solely from a teflon diffuser). To avoid saturation, the detector was operated in high-capacity mode, leading to direct sun spectra of high spectral noise. In June 2023 an additional neutral-density optical filter was installed in combination with the (existing) diffuser to enhance attenuation, so the detector was reverted to its default low-noise mode of operation. In January 2024, a second filter/diffuser setup with the addition of a HOYA U340 bandpass filter was installed on a different position of the filter-wheel, to eliminate wavelengths longer than ~ 390 nm, thus reducing the effect of stray-light on the DOAS retrievals in the UV. Since then, direct sun measurements are repeated twice, once with and once without the U340 filter, each with an integration time of 30 sec. In the end of May 2024, Delta was uninstalled and transported to Cabauw, the Netherlands, to participate in the third Cabauw Intercomparison of UV-Vis DOAS Instruments (CINDI-3) intercomparison campaign (https://actris.eu/news-events/news/cindi-3-extensive-air-pollution-measurement-campaign-cabauw, last access: 8 November 2025). The instrument returned to its operational site at LAP.AUTH at the end of June 2024, but with a shift in the wavelength calibration, probably due to stress of the mechanical parts of the spectrograph during transportation. In this study, we focus only on direct sun measurements performed by Delta during the period June 2023 to May 2024, when the instrument was stable and fully operational, thereby avoiding potential biases in the comparison with Brewer and Pandora due to different instrument states.

2.3 Brewer

The Brewer spectrophotometer (SN #005) that was used in this work is a MKII single-monochromator instrument that was installed at LAP.AUTH in 1982 (Figure 1). It is still fully operational and regularly records total ozone, sulfur dioxide (SO_2) as well as spectral UV in the wavelength range 290 – 330 nm and aerosol optical depth at selected wavelengths (Meleti and Cappellani, 2000; Gröbner and Meleti, 2004). Regular calibrations for TOC are conducted via participation to intercomparison campaigns organized by the European Regional Brewer Calibration Center (RBCC-E) (e.g., Redondas et al., 2018). The last calibration against the RBCC-E standard was performed in 2021 (WMO, 2024). Strict quality control protocols ensure the

https://doi.org/10.5194/egusphere-2025-5627
Preprint. Discussion started: 5 January 2026

validity of Brewer observations, which are made available to the scientific community through the channels of the World Meteorological Organization's World Ozone and Ultraviolet Radiation Data Centre (WOUDC, https://woudc.org/, last access: 8 November 2025) and the European Brewer Network (EUBREWNET, https://eubrewnet.aemet.es/eubrewnet/, last access: 8 November 2025), a database established under COST Action ES1207, where TOC and spectral UV measurements are available in (almost) near-real time. The extensive time series of Brewer TOC observations at LAP.AUTH has been widely used in scientific research studies regarding the long-term variability and trends of TOC and in satellite validation studies (e.g., Bais et al., 1993; Meleti et al., 2009; Fragkos et al., 2016; Fountoulakis et al., 2019b; Amiridis et al., 2024; Garane et al., 2024). The retrieval method of total ozone column from Brewer measurements follows the established methodology described in Kerr et al., (1981). It is based on direct solar spectral irradiance measured simultaneously at four UV wavelengths (310.1, 313.5, 316.8 and 320.0 nm) and utilizes the Bass and Paur, (1985) ozone absorption cross sections. Furthermore, the retrieval algorithm assumes an effective ozone absorption temperature of 44°C and an effective ozone height of 22 km. The estimated uncertainty of the Brewer TOC observations is nominally about 1% (Kerr et al., 1988).

2.4 Pandora

Pandora is a dual-spectrometer system that was collaboratively designed by the National Aeronautics and Space Administration (NASA), the European Space Agency (ESA), SciGlob Instruments and Services (https://sciglob.com/, last access: 8 November 2025) and Luftblick OG. It aims to improve and extend the capabilities of the ground-based infrastructure for satellite validation. To support this mission, the large-scale global monitoring network, PGN, was developed. PGN provides homogeneous instrument calibration, central data processing and formatting, and quick delivery of final data products. It focuses on the monitoring of air-quality-related species and delivers DS-DOAS total column and MAX-DOAS tropospheric column and surface concentration measurements of several trace gases, including NO_2, O_3, formaldehyde (HCHO), water vapor (H_2O) and SO_2 (e.g., Herman et al., 2009), with a high temporal resolution. Pandora instruments have not only been involved in satellite validation activities (e.g., Judd et al., 2020; Verhoelst et al., 2021), but have also been employed in the assessment of air pollution and for understanding of the physical and chemical processes in the atmosphere (e.g., Tzortziou et al., 2015; Spinei et al., 2018; Robinson et al., 2020). One such instrument (Pandora #240) has been installed at LAP.AUTH in September 2022. The system consists of two commercial spectrometers by Avantes (https://www.avantes.com/, last access: 8 November 2025), housed in a thermally isolated box for temperature stabilization, covering the UV-VIS and NIR regions, respectively. The operational TOC product is retrieved from the UV-VIS spectrometer, which features a symmetrical Czerny-Turner design with a grating of 1200 lines mm^{-1} and a 50 μm entrance slit. The spectrometer is equipped with a back-thinned Hamamatsu CCD detector of 2048×64 pixels, recording spectra in the range 277–538 nm with a resolution of approximately 0.55 nm FWHM (Herman et al., 2015). The TOC retrieval methodology using DS-DOAS, along with the Algorithm Theoretical Baseline Document (ATBD) and usage guidelines, are described in detail in the corresponding manuals that are publicly available through the official PGN website (https://www.pandonia-global-network.org/home/documents/manuals/, last access: 8 November 2025). Here we use the Pandora TOC product (version 1.8.49), which is publicly available through

https://doi.org/10.5194/egusphere-2025-5627
Preprint. Discussion started: 5 January 2026

the official PGN website. The operational products of PGN include a quality flag for the retrievals, as part of the standard data quality control and in this study, only medium- and high-quality TOC data are used. Throughout the study period, the instrument remained fully operational, with minimal gaps in its timeseries due to routine maintenance.

3 Methodology

3.1 DOAS-based TOC retrieval algorithm

This section deals with the TOC retrieval algorithm that is based on the application of DOAS on direct sun spectra measured by Delta. DOAS relies on the modified Beer - Lambert law, which describes the attenuation of solar radiation in the atmosphere by molecular and aerosol absorption and scattering. DOAS is based on the principle that molecular and aerosol extinction processes, various trace gas absorptions, as well as instrumental and turbulence effects show broad spectral features, while certain trace gases exhibit narrow absorption structures. Of key importance in the DOAS principle to detect and quantify trace gases in the atmosphere is the separation of the narrow-band absorptions from the broad-band spectral features, with the latter (including Rayleigh and aerosol extinction) being approximated by fitting a low-order polynomial function.

The TOC retrieval algorithm involves a two-step process. First, a least squares fit is performed within a defined spectral window to calculate the O_3 slant column densities (SCD), i.e., its concentration integrated along the light path. This process is usually referred to as DOAS fit. In the DOAS analysis, however, SCDs are retrieved with respect to a reference spectrum, also called Fraunhofer Reference Spectrum (FRS). Since FRS can also be influenced by trace gas absorptions, the primary output of the DOAS analysis is the differential slant column density (dSCD), defined as the difference between the SCD of the analyzed spectrum and that of the FRS (SCD_{FRS}):

$$dSCD = SCD - SCD_{FRS} \quad (1)$$

The FRS is usually a single spectrum, or the average of multiple spectra measured under clear-sky conditions. In order to obtain high absorption signals in the DOAS analysis, the effect of O_3 absorption should be minimal in the reference spectrum. Hence, the aim is to select a reference spectrum in a day when TOC is relatively small, measured under the shortest possible slant path (or small SZA). In this study, the chosen FRS is a spectrum recorded by the same instrument at LAP.AUTH on 06 May 2024, at SZA=23.9°. The reference spectra are slightly different for the UV and VIS retrievals, as they were measured with a small temporal offset of approximately 30 sec, as discussed in Sect. 2.2. An important benefit of using an FRS recorded with the same instrument is the precise wavelength alignment, thus ensuring effective removal of both the Fraunhofer absorption features of solar radiation and any characteristic features in the instrument's spectral response. Solar irradiance data measured by pyranometers in Thessaloniki (Supplement Sect. S1) confirm clear-sky conditions during the whole day, except for a brief 30-minute period after 14:00 UTC, however this is not a concern, as the FRS was recorded around local noon at approximately 10:30 UTC.

The second step of the retrieval algorithm is the conversion from O_3 SCD to VCD, by division with an AMF, according to Eq. (2).

https://doi.org/10.5194/egusphere-2025-5627
Preprint. Discussion started: 5 January 2026

$$VCD = \frac{SCD}{AMF} \quad (2)$$

Given that VCD equals TOC in this case, the combination of Eq. (1) and (2) yields:

$$TOC \equiv VCD = \frac{dSCD + SCD_{FRS}}{AMF} \quad (3)$$

In the following subsections, a description is given of the DOAS settings that are applied for the retrieval of O_3 SCDs in the Huggins and Chappuis bands, the calculation of the AMFs that are required for the conversion to VCDs, and the calibration procedures applied for the estimation of the O_3 SCD of the reference spectrum.

3.2 DOAS retrieval settings

Ozone dSCDs are retrieved separately in the UV and VIS spectral ranges. In both cases, the retrieval settings are based on recommendations of NDACC (Hendrick et al., 2011) and the Fiducial Reference Measurements for Ground-Based DOAS Air-Quality Observations (FRM4DOAS) project (Van Roozendael et al., 2024), as well as on results from the CINDI-2 campaign (https://uv-vis.aeronomie.be/groundbased/campaigns/CINDI2camp.php, last access: 8 November 2025) (e.g., Kreher et al., 2020) with some adaptations based on the specific instrumentation. While the NDACC recommendation for ozone retrievals in the Chappuis bands is to use a spectral window of up to 540 nm (Hendrick et al., 2011) since uncertainties of ozone fitting are minimal, the spectrograph of Delta has shorter spectral coverage. Hence, the spectral window was set from 450 to 520 nm to cover a large enough wavelength range, in which ozone exhibits absorption features, without stretching the spectrograph to its upper spectral limit (523 nm), where ozone features are anyway broadband. This spectral window was also recommended during the CINDI-2 campaign (Kreher et al., 2020). In the UV, the ozone absorption cross section shows a significant temperature dependence (Serdyuchenko et al., 2014). To account for this effect, a linearization approach is applied by including two ozone absorption cross sections in the DOAS fit: one at 223 K, representative for stratospheric temperatures, and one temperature-differential cross section (obtained as the difference between cross sections at 243 K and 223 K). Moreover, for the retrieval in the Chappuis bands, no I_0-correction has been applied since the ozone cross section structures in this region are broad and such a correction has a negligible effect on the retrieved dSCDs, which was also confirmed by a sensitivity test. A third- and fifth-order polynomial is used to fit the low frequency structures due to molecular and Mie scattering in the UV and VIS ranges, respectively, and a first-order polynomial to account for stray-light effects through an intensity offset term. While in MAX-DOAS retrievals an additional pseudo cross section is usually included in the DOAS fitting to account for the Ring effect in the scattered radiation spectra, DS-DOAS is based on direct radiance spectra and thus such cross section is not included in the analysis.

The recorded spectra are analyzed using the QDOAS (version 3.6.0, December 2023) software developed at BIRA-IASB (https://uv-vis.aeronomie.be/software/QDOAS/, last access: 8 November 2025). The slit function parameters, as well as any shift of the wavelength calibration of the measured spectra are fitted by QDOAS using a high-resolution solar FRS (Chance

https://doi.org/10.5194/egusphere-2025-5627
Preprint. Discussion started: 5 January 2026

and Kurucz, 2010) prior to the DOAS analysis. The retrieval settings of O_3 in the UV and VIS ranges, as well as the trace gas absorption cross sections that are included in the DOAS fit are summarized in Table 1.

Table 1: Retrieval settings used for the retrieval of ozone dSCDs in the UV and VIS spectral ranges.

Parameter	Data source	O_3 retrieval	
		Huggins bands (UV)	Chappuis bands (VIS)
Wavelength range		320 – 340 nm	450 – 520 nm
O_3 (223 K)	Serdyuchenko et al., (2014)	✓ I_0-corrected (SCD of 10^{20} molec. cm^{-2}) and Taylor terms (Puķīte et al., 2010)	✓
O_3 (243 K)	Serdyuchenko et al., (2014)	✓ I_0-corrected (SCD of 10^{20} molec. cm^{-2}), subtracted from O_3 (223 K)	✓ Orthogonalized to O_3 (223 K)
NO_2 (298 K)	Vandaele et al., (1998)	✓ I_0-corrected (SCD of 10^{17} molec. cm^{-2})	✓ I_0-corrected (SCD of 10^{17} molec. cm^{-2})
NO_2 (220 K)	Vandaele et al., (1998)		✓ I_0-corrected (SCD of 10^{17} molec. cm^{-2}) and orthogonalized to NO_2 (298 K)
O_4 (293 K)	Thalman and Volkamer, (2013)		✓
O_4 (203 K)	Thalman and Volkamer, (2013)		✓ Orthogonalized to O_4 (293 K)
HCHO (298 K)	Meller and Moortgat, (2000)	✓	
H_2O (293 K)	HITEMP (Rothman et al., 2010)		✓
Polynomial degree		Order 3	Order 5
Intensity offset		Order 1	Order 1
Wavelength Calibration	Based on a high-resolution solar reference spectrum (Chance and Kurucz, 2010)		

Figure 2 shows a typical DOAS fit example of O_3 in the UV and VIS for two consecutive direct sun spectra (with a time difference of ~ 30 sec) measured by Delta on 30 March 2024 at 13:57 UTC and at 58.6° SZA, with and without the U340

https://doi.org/10.5194/egusphere-2025-5627
Preprint. Discussion started: 5 January 2026

bandpass filter. Only the trace gas fits that are common for the UV and VIS retrievals are presented in Figure 2. The ozone dSCDs retrieved from the two channels are in very good agreement, with a relative difference of ~0.45%. The DOAS fit of O_3 is better in the UV due to the stronger absorption in the Huggins bands, leading to differential optical depths of about one order of magnitude higher. Nevertheless, the ozone fitting in the VIS provides consistent and reliable results, with the retrieval accurately resolving the three main absorption bands in the selected wavelength range. The root mean square (RMS) of the DOAS fit residual in the VIS (in this example 1.18×10^{-4}) is significantly lower than in the UV (4.32×10^{-4}), by a factor of approximately 4, primarily due to the higher SNRs in the visible range. However, this behavior is not limited to individual cases. Figure S2 (Supplement Sect. S2) shows that RMS values in the VIS range are generally lower than those in the UV. Moreover, the increase of RMS with increasing SZA is less pronounced in the VIS, whereas in the UV retrievals RMS exhibits a stronger increase, indicating higher sensitivity to stray-light effects in the Huggins bands under low solar elevations. NO_2 is more accurately captured in the VIS, because of its pronounced narrow-band absorption features compared to the UV range, where also the attenuation of solar radiation is dominated by ozone absorption.

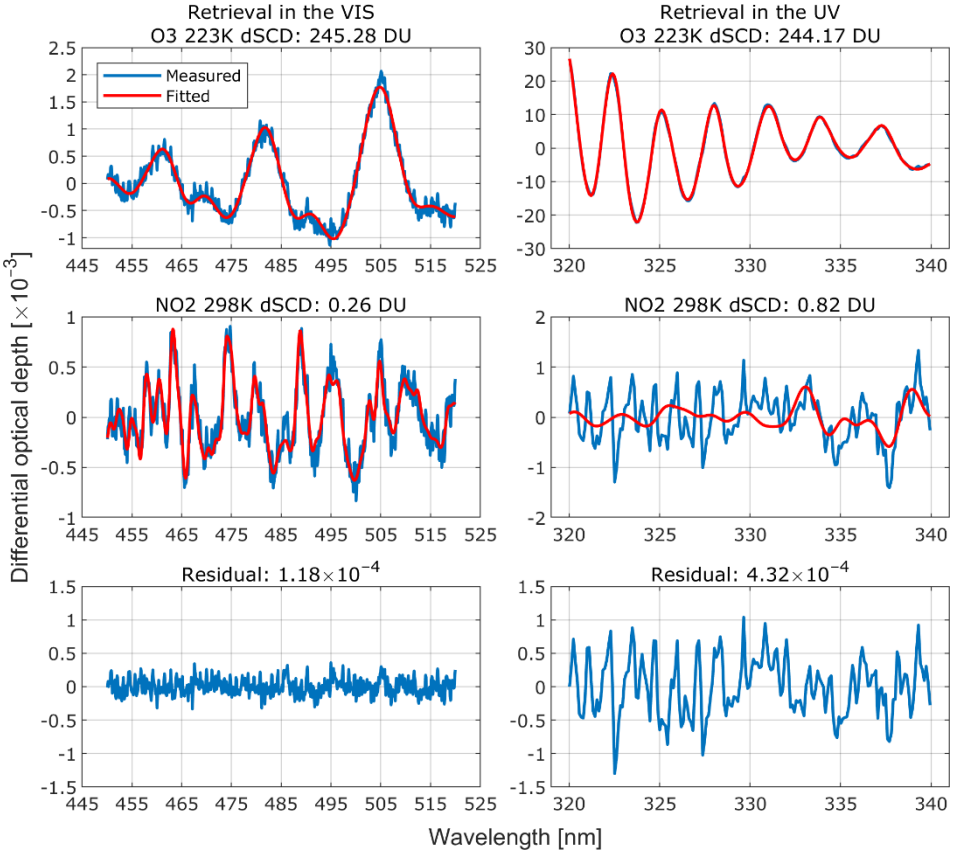

Figure 2: Example of DOAS spectral fitting for ozone in the VIS (left column) and UV (right column) spectral ranges. The top panels show the measured (blue) and fitted (red) differential optical depths for O_3, the middle panels for NO_2, and the bottom panels the corresponding fitting residuals.

https://doi.org/10.5194/egusphere-2025-5627
Preprint. Discussion started: 5 January 2026

3.3 AMF calculation

The AMF represents the relative path length that solar radiation follows through the atmosphere compared to the vertical path. For direct sun observations, the AMF can be geometrically approximated by $\sec SZA = 1/\cos SZA$. While this approach is relatively accurate for gases located in the lowermost layers of the atmosphere and for small SZAs, it does not account for the Earth's curvature which introduces a dependency on the vertical distribution of the absorbing species. For ozone, which is predominantly concentrated in the stratosphere, this simplistic approximation can lead to significant errors in AMF calculations, which are directly propagated to TOC given their linear relationship as described by Eq. (2). In this study, we adopt for the AMF calculation the formula presented in Cede et al., (2006), i.e.,

$$AMF = \sec\left[\arcsin\left(\frac{R}{R + h_{eff}} \cdot \sin SZA\right)\right] \quad (4)$$

where R is the Earth's radius (6370 km) and h_{eff} is the effective height of the ozone layer, which has a latitudinal gradient with a seasonal variability. For more precise AMF calculations we used the publicly available (https://avdc.gsfc.nasa.gov/, last access: 8 November 2025) atmospheric ozone profile climatology by Ziemke et al., (2021) which has been constructed by combining daytime ozone profiles from the Aura Microwave Limb Sounder (MLS) and Modern-Era Retrospective Analysis for Research Applications version 2 (MERRA-2) Global Modeling Initiative (GMI) model simulations, binned to latitude bands of 5°. The ozone effective height was calculated on a monthly basis using Eq. (5) as in Gröbner et al., (2021):

$$h_{eff} = \frac{\int z \cdot c(z) dz}{\int c(z) dz} \quad (5)$$

where $c(z)$ is the concentration of O_3 as a function of altitude, z.

Figure 3 shows the seasonal variability of h_{eff} for the latitude bands of 35°N – 40°N and 40°N – 45°N (blue and green lines, respectively). Since the latitude of our monitoring station is at the edge of these bands, the mean h_{eff} from both bands (red line) has been considered as more representative. The ozone profile climatology data reveal a distinct seasonal pattern with h_{eff} reaching a minimum of 22.3 km in winter (February) and gradually increasing through summer, reaching an autumn peak (in September) of 23.8 km. If a temporally constant h_{eff} of 23 km were applied in Eq. (4), the impact on the calculated AMFs would be negligible for SZAs less than 70° (within ±0.1%), however, at higher SZAs, this assumption would introduce an error of up to 0.8%.

https://doi.org/10.5194/egusphere-2025-5627
Preprint. Discussion started: 5 January 2026

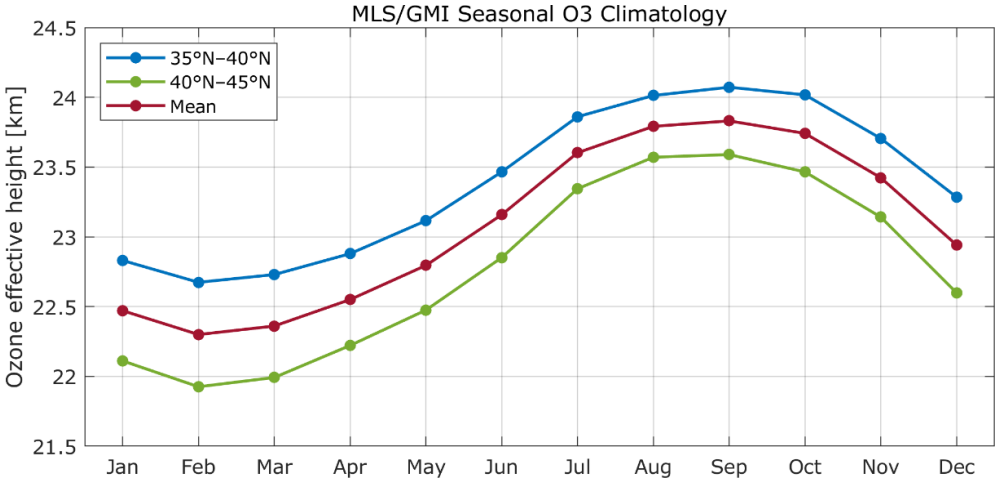

Figure 3: Seasonal climatology of ozone effective height derived from MLS/GMI data for the latitude bands 35°N–40°N (blue) and 40°N–45°N (green), along with their mean (red), which is considered more representative for the latitude of LAP.AUTH.

3.4 Estimation of the O_3 SCD of the reference spectrum

According to Eq. (3), TOC calculations require knowledge of the absolute slant column of the reference spectrum (SCD_{FRS}). This calibration procedure is performed using two approaches, i.e., the Langley Extrapolation (LE) method (Gröbner and Kerr, 2001) and the Bootstrap-Estimation (BE) method, as described in Cede et al., (2006) and in Herman et al., (2009). In the former case, O_3 dSCDs are measured during a day (or days) at different SZAs, corresponding to different AMFs and SCD_{FRS} is calculated by extrapolating the differential O_3 slant column to zero AMF. On 21 June 2023, Delta was configured to record only direct sun spectra with a high sampling rate (integration time of 30 sec) from sunrise to sunset. This day was chosen not only due to cloud-free conditions (Supplement Sect. S1), but also due to the wide range of SZAs covered. One of the most important conditions that need to be met for a proper application of LE is that TOC is constant throughout the day, ensuring a linear relationship between O_3 dSCDs and AMF. Based on Brewer and Pandora TOC measurements on that day, it was found that TOC was relatively constant around noon and evening up to 75° SZA, followed by a gradual decrease in TOC levels afterwards (not shown here). Even though measurements in the early morning were also characterized by cloud-free conditions, the O_3 dSCDs could not be retrieved because the direct sun direction was blocked by buildings in the campus. Hence, only data recorded between 10:30 – 16:00 UTC have been used for the LE method. The SZA limitation reduces the AMF range, but the high sampling rate allows for statistically robust results. Figure 4a shows the O_3 dSCDs on 21 June 2023 as a function of the AMF. The Pearson's correlation coefficient is very close to unity (R^2>0.999), revealing a very consistent linear relationship. The extrapolation to AMF=0 (i.e., the intercept of the linear regression) yields $SCD_{FRS} = 410.766\ DU$.

The Bootstrap-Estimation method is another technique that can be used for the calculation of SCD_{FRS}, however, this method is only applicable when a large number of O_3 dSCD data is available, measured on different days and for a wide range of AMFs and TOCs, to provide statistically robust results. Figure 4b shows the O_3 dSCDs from the VIS range for the whole period of study against the respective AMFs. The O_3 data are grouped in narrow AMF bins of 0.2, and for each group the 3rd

https://doi.org/10.5194/egusphere-2025-5627
Preprint. Discussion started: 5 January 2026

345 percentile of the distribution is calculated, corresponding to the minimum measured dSCD for the respective AMF bin. To minimize uncertainties in the calculated AMF and to remove O_3 data measured at very high SZA, the analysis is limited to AMFs lower than 5.5. Like in the LE method, the minimum O_3 dSCDs are linearly fitted to estimate the intercept of the regression that corresponds to the O_3 slant column of the reference spectrum. In this case, the SCD_{FRS} was found to be 409.054 DU, which is in very good agreement with the one calculated with the LE method. For the TOC calculations, the SCD_{FRS} that 350 is used in Eq. (3) is the mean of the two methods, i.e., $SCD_{FRS} = 409.91\ DU$. When the same methodology is applied to data in the UV range (results not shown here), the findings are consistent with the VIS retrievals, with $SCD_{FRS} = 409.16\ DU$. However, in the UV range, to ensure statistical robustness, the AMF range was restricted to values below 4, since at larger SZAs the RMS filtering that is applied (see Sect. 4) removes a substantial number of measurements. Even though the estimation of the O_3 SCD of the reference spectrum was based solely on retrievals in the VIS (data in the UV are not available on 21 June 355 2023 as noted in Sect. 2.2), the small temporal difference between the UV and VIS reference spectra ensures that atmospheric variations are negligible and hence the same SCD_{FRS} is applied to both UV and VIS data.

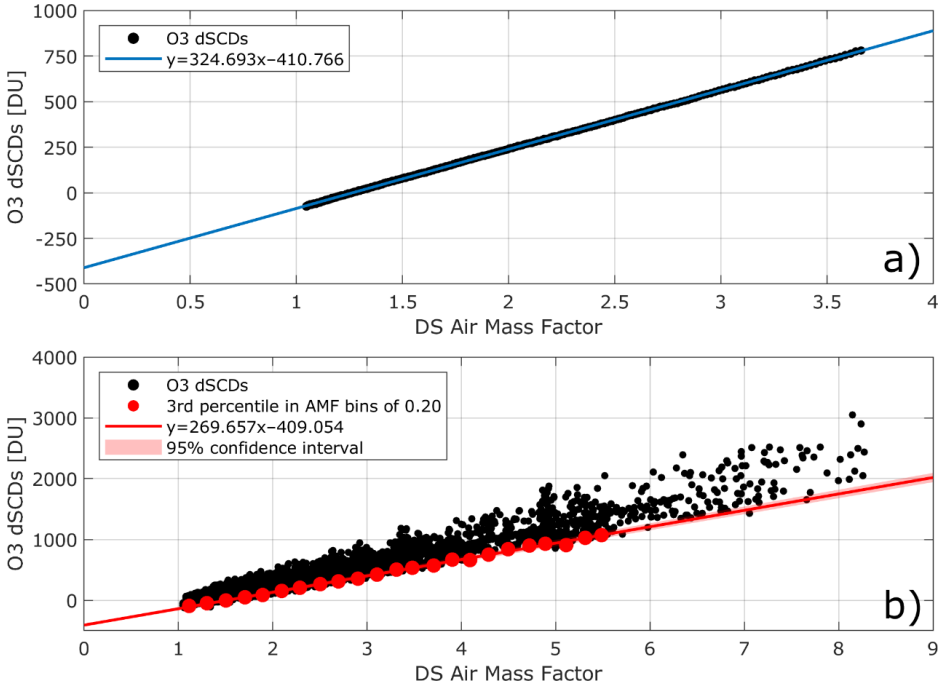

Figure 4: (a) Example of a single clear-sky day Langley plot showing O_3 dSCDs as a function of AMF. (b) Bootstrap-Estimation analysis over the whole dataset, where black markers represent all O_3 dSCDs and red markers correspond to the 3rd percentiles 360 **within AMF bins of 0.20.**

4 Results and discussion

This section presents the results of TOC retrievals in the UV and VIS spectral ranges, including an intercomparison of data from the two channels, as well as comparison and validation against collocated measurements from the Brewer and Pandora

https://doi.org/10.5194/egusphere-2025-5627
Preprint. Discussion started: 5 January 2026

instruments, which here are considered reference instruments because of their proven measurement quality and much longer history in TOC monitoring.

It should be noted that no direct cloud flagging algorithm is applied to the data measured by Delta. Only a coarse cloud-filtering procedure is implemented, based on the calculated exposure time of the CCD camera, to reject highly contaminated measurements. During the instrument's operation the exposure time is automatically adjusted to optimize the signal strength while preventing spectral saturation. When the calculated exposure time exceeds the threshold value of 4 sec, direct sun measurements are aborted. While this approach effectively eliminates measurements under thick cloud conditions, measurements are still performed under thin clouds, potentially introducing at some degree cloud-related contamination. To ensure high-quality DOAS fits and to minimize errors due to weak radiation levels, the data are additionally filtered based on the SZA (measurements at SZAs greater than 85° are excluded from the analysis), as well as on the RMS of the DOAS fit residuals. Different threshold values are applied for the UV and VIS spectral regions, to account for their SNR differences, as previously discussed in Sect. 3.2. The peaks of the frequency distribution of the DOAS fit RMS over the whole datasets are approximately 5×10^{-4} and 1.5×10^{-4} in the UV and VIS, respectively. In the UV channel, even though an RMS threshold of 1×10^{-3} ensures good-quality DOAS fits, it removes almost all data measured at SZAs higher than 70°. Hence, in order to retain measurements up to at least 80° SZA, the RMS threshold was adjusted to 2×10^{-3} as in Kumar et al., (2020). Due to the lower O_3 optical depths in the VIS channel, the RMS threshold was set to 4×10^{-4}, which, while stricter than for the UV channel, ensures accurate fits. These threshold values remove 7.1% and 10.4% of the O_3 retrievals measured at SZAs lower than 85°, in the UV and VIS ranges, respectively.

4.1 Comparison of UV and VIS TOC retrievals

Figure 5 shows the comparison of ozone absolute slant column densities (calculated using Eq. (2) by multiplying TOC with its corresponding AMF) retrieved from Delta UV and VIS spectra over the whole period of study.

https://doi.org/10.5194/egusphere-2025-5627
Preprint. Discussion started: 5 January 2026

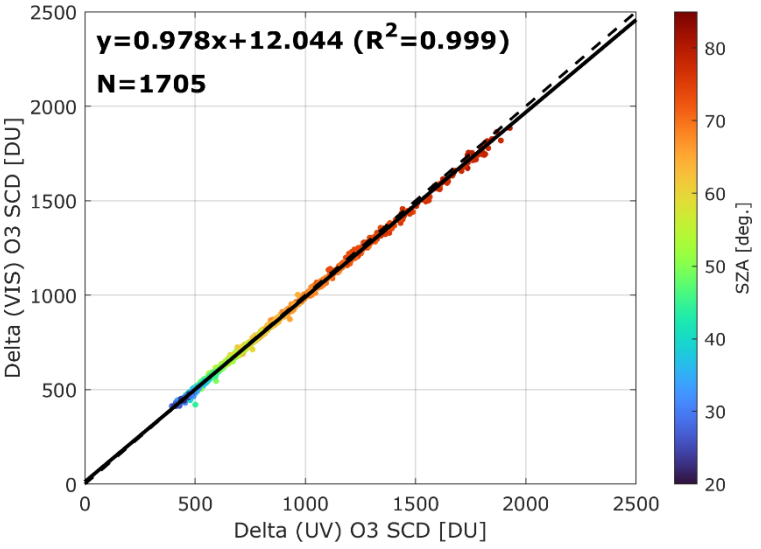

Figure 5: Comparison of ozone SCDs retrieved from Delta UV and VIS spectra over the study period. The data are color-coded by SZA. The dashed line represents the 1:1 reference, while the solid line shows the linear regression fit.

The two datasets show an almost perfect linear correlation (R^2=0.999), that highlights the consistency of the DOAS retrievals across the UV and VIS spectral windows. The data are color-coded by SZA, indicating that the good agreement applies to the full SZA range, from about 17° up to 85°. The higher O_3 SCDs observed at large SZAs do not necessarily correspond to increased TOC but rather reflect the longer atmospheric light paths of radiation. At smaller SZAs the scatter is minimal, while a slight increase appears at larger SZAs. This behavior is consistent with the reduced signal strength in the UV, as well as the stronger influence of stray light under such conditions. Despite these effects, no strong systematic SZA-dependent bias is evident, supporting the robustness of both retrievals. Overall, the comparison suggests that the Delta instrument can deliver reliable and consistent ozone SCD measurements in both spectral regions, supporting the feasibility of using the Chappuis bands for TOC retrievals, thereby complementing the traditional UV-based approaches. The regression's slope indicates a small systematic bias of approximately 2% between UV and VIS O_3 SCDs, which highlights the strong consistency between the retrievals in two spectral regions.

The corresponding comparison of TOC measurements, derived from the UV and VIS channels of Delta over the study period is presented in Figure 6. Compared to the O_3 SCDs, the dynamic range of the TOC values is significantly smaller, which statistically leads to a weaker correlation between the two datasets. Nevertheless, the scatter plot (left panel) indicates a very strong correlation between the two datasets, with a high Pearson's correlation coefficient (R^2=0.975). Most of the data points are close to the 1:1 line (dashed black), indicating high agreement between TOC values obtained from the two channels. The data are color-coded by the O_3 dSCD, which represents the strength of the ozone differential absorption signal. Data points exhibiting significant deviations from the 1:1 line, as well as most of the outliers, are associated with very low O_3 differential optical depths, which increase the noise in the visible measurements, as the ozone absorption signal becomes weak under such conditions. The linear regression yields a slope of 0.957 and an intercept of 14.922 DU, suggesting a slight systematic

https://doi.org/10.5194/egusphere-2025-5627
Preprint. Discussion started: 5 January 2026

deviation. The histogram (right panel) illustrates the frequency distribution of TOC percentage differences between the VIS and UV channels. The distribution is closely approximated by a gaussian, with a median and mean differences of –0.44% and –0.39%, respectively, indicating a slight negative bias for the VIS channel. Most of the differences fall within a relatively narrow range of approximately ±2%, as defined by the 5th and 95th percentiles (green lines). Additionally, the interquartile range (magenta lines) further highlights that 50% of the data falls within a narrower band around the median (within –1 and 0.5%). The high correlation and the narrow spread of differences confirm the robustness of DS-DOAS in retrieving TOC across both spectral regions and provide the general overview of their comparison. In the following subsection, the TOC data from both channels of Delta are compared and validated with respective O_3 data from Brewer and Pandora.

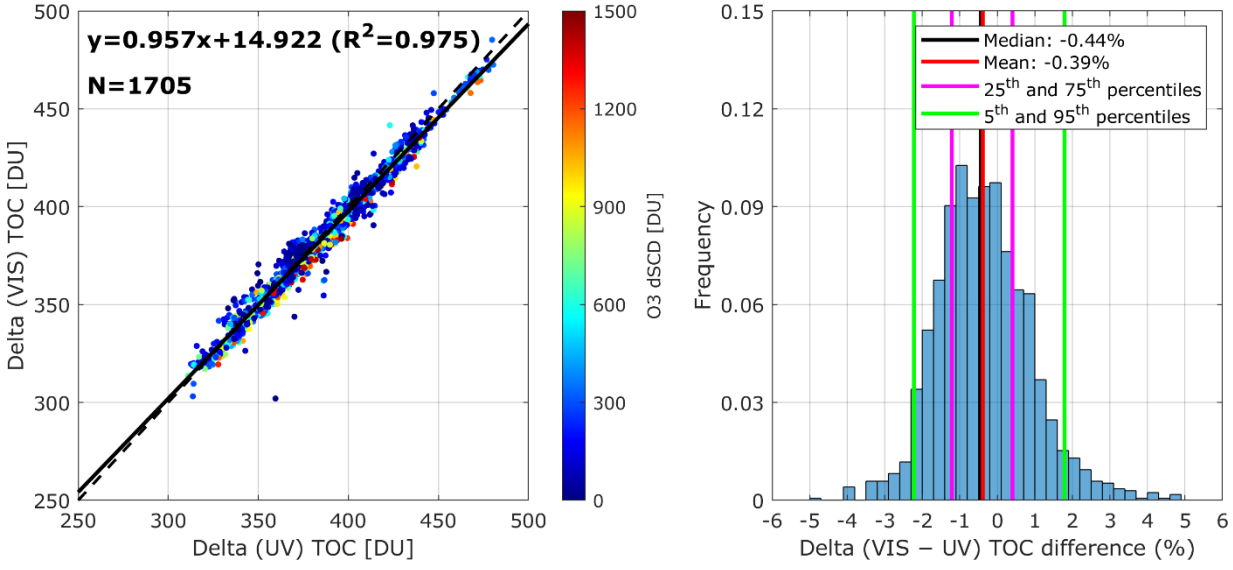

Figure 6: Comparison of TOC measurements from the UV and VIS channels of Delta over the study period. (a) Scatter plot of VIS against UV retrievals, color-coded by ozone dSCDs. The dashed line represents the 1:1 reference, while the solid line shows the linear regression fit. (b) Frequency distribution of their respective percentage differences (VIS–UV). The vertical lines indicate the median (black), mean (red), the 25th and 75th percentiles (magenta), and the 5th and 95th percentiles (green).

4.2 Intercomparison with the Brewer and Pandora

For the intercomparison, collocated TOC measurements from Delta, Brewer, and Pandora were identified using a temporal matching criterion of ±10 minutes between observations. This temporal window was selected to balance the need for sufficient data pairs with the requirement to minimize short-term atmospheric variability and to avoid large AMF differences, particularly at high SZAs.

Figure 7 presents the intercomparison of ozone SCDs from Delta with Brewer (left panels) and Pandora (right panels) data, for both VIS (top) and UV (bottom) retrievals. Like in Sect. 3 the O_3 SCDs have been calculated using Eq. (2). In all cases, the correlation is exceptionally high ($R^2 > 0.98$), with slopes close to unity and intercepts of a few DU. This confirms that the Delta SCDs from both channels are fully consistent with those derived from the reference instruments across the full dynamic range of observations. The color coding that follows the SZAs shows that the agreement is maintained throughout the range

https://doi.org/10.5194/egusphere-2025-5627
Preprint. Discussion started: 5 January 2026

of viewing geometries, although the scatter is significantly larger at large SZAs (> 70°). Notably, small differences between instruments may arise not only from instrumental characteristics and retrieval methodologies, but also from their different sampling strategies. For instance, Delta records direct sun spectra with an integration time of ~30 s, while a single Brewer measurement requires ~3 minutes, leading to slightly different AMFs being assigned to the observations. In addition, the Brewer software calculates the AMF for a constant effective ozone height which can introduce minor differences in the SCD calculation. Further discrepancies among the three instruments may also arise from differences in the TOC retrieval settings. Brewer TOCs are derived from measurements at four discrete wavelengths in the range 310-320 nm, an approach that minimises the sensitivity to ozone temperature changes but also inherently limits spectral redundancy relative to multi-wavelength DOAS retrievals. Moreover, Delta in the UV employs the 320–340 nm region (Sect. 3.2), while Pandora applies a DOAS fit over the 305–325 nm spectral window, which may also introduce differences in the retrieved TOC, as the sensitivity to ozone absorption structures varies across these ranges. Finally, the ozone absorption cross sections used for the TOC retrieval from each instrument may also introduce discrepancies. As mentioned in Sec. 3.2, the TOC retrieval from Delta is based on Serdyuchenko et al., (2014) O_3 cross sections, which are also used in the Pandora retrieval algorithm. The Brewer TOC data that are used in this study are based on Paur and Bass (1985) cross sections which result in higher TOC, on average 0.8%, than with Serdyuchenko et al., (2014) cross sections (Fragkos et al., 2015).

As outlined in Sect. 2.2, the VIS measurements span the period from June 2023 to May 2024 (~11 months), whereas the UV measurements became operational in January 2024 (~6 months of coverage), hence, the number of available collocations in the UV datasets is smaller than in the VIS. This limitation, however, does not affect the objectives of this study, which focuses on the investigation and robustness of VIS-based retrievals rather than assessing long-term variability of TOC. Moreover, the six-month UV record covers the period of the year when ozone exhibits its strongest variability in Thessaloniki (Zerefos et al., 1998; Fragkos et al., 2016), thereby including both low and high TOC values, even though the full seasonal cycle is not captured. The linear regressions indicate negligible systematic biases, which are within the typical uncertainties of DOAS retrievals and do not show a pronounced dependence on SZA. Overall, the good agreement of Delta with both Brewer and Pandora at the SCD level provides a strong basis for the subsequent TOC intercomparisons presented in this section.

https://doi.org/10.5194/egusphere-2025-5627
Preprint. Discussion started: 5 January 2026

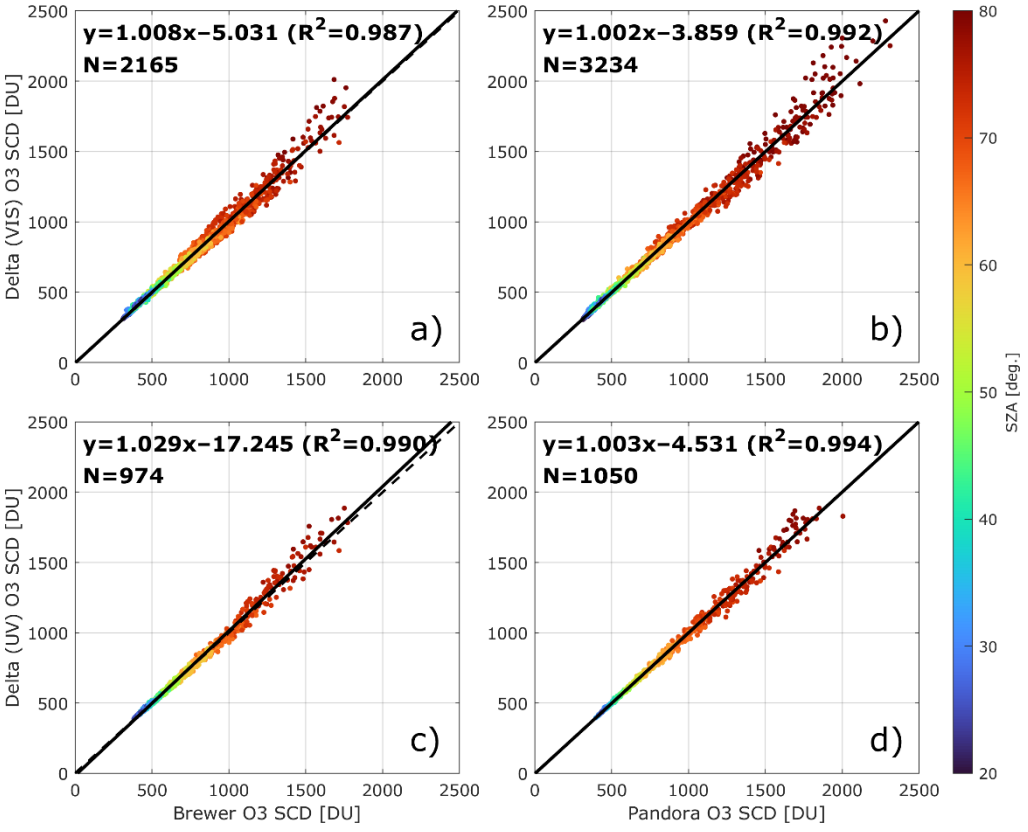

Figure 7: Intercomparison of ozone SCDs retrieved by Delta against Brewer and Pandora instruments. Panels (a) and (c): Delta VIS and Delta UV compared to the Brewer, respectively. Panels (b) and (d): Delta VIS and Delta UV compared to the Pandora, respectively. Data points are color-coded by SZA. The dashed lines indicate the 1:1 reference, while the solid lines show the fitted regression.

Figure 8 presents the comparison of TOC measurements from Delta (VIS shown on the top row and UV at the bottom) with collocated Brewer observations. Both comparisons show very good agreement, with very high correlation coefficients (R^2=0.986 for the VIS and R^2=0.985 for the UV, respectively). The regression slopes are close to unity (0.981 for VIS and 0.999 for UV, respectively), while the intercepts remain small (up to 6 DU for VIS), indicating minor systematic deviations. The scatter plots confirm that most points are closely aligned with the 1:1 line, with only limited spread. It should be noted that in the Delta UV dataset, the lowest TOC values are missing, since the available six-month record does not cover the October–November period, when ozone concentrations typically reach their annual minimum over Thessaloniki (Garane et al., 2024). The histograms of percentage differences (Delta–Brewer) further highlight the consistency of the datasets. For the Delta (VIS)–Brewer comparison (panel a), the mean and median biases are –0.08% and –0.18%, respectively, with most differences falling within ±2% (5^{th}–95^{th} percentiles). For the Delta (UV)–Brewer comparison (panel b), the distribution is slightly asymmetric, while the mean and median biases are 0.24% and 0.08%, and with the majority of the differences confined to within ±2%. The interquartile ranges (magenta lines) indicate that half of the data lie within a very narrow band (<1%) around the median in both cases. The narrower interquartile range in the UV comparison suggests a slightly better overall

https://doi.org/10.5194/egusphere-2025-5627
Preprint. Discussion started: 5 January 2026

agreement with the Brewer relative to the VIS retrievals, although in both cases the differences remain well within the expected uncertainty of DS TOC measurements.

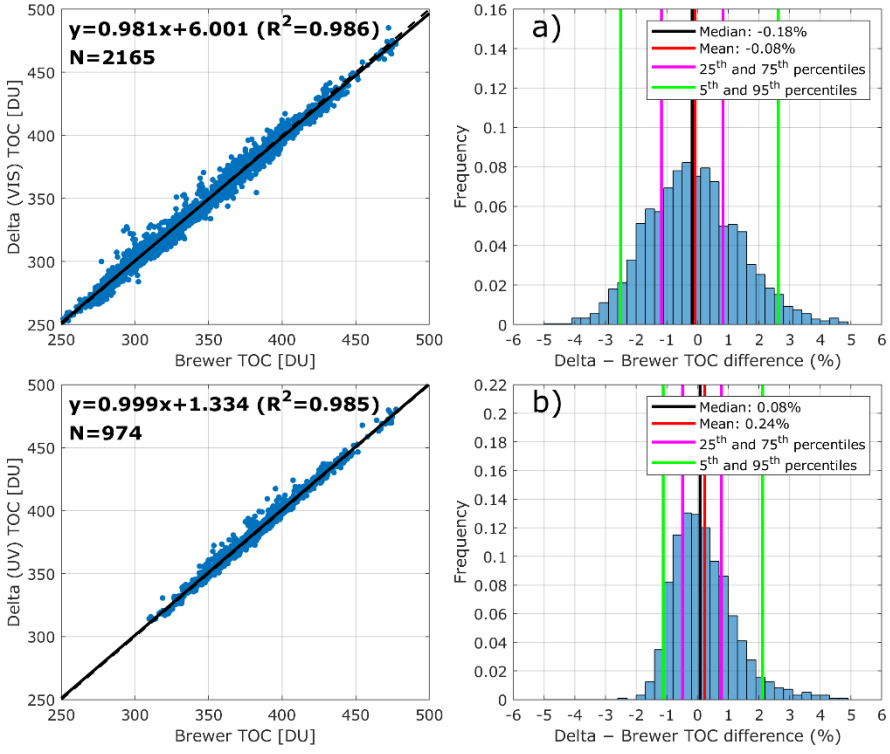

Figure 8: Comparison of TOC measurements from Delta and the Brewer. The left panels show scatter plots of collocated TOC retrievals from Delta VIS (top panel) and Delta UV (bottom panel), with regression fits (solid line) and the 1:1 reference (dashed line). The right panels show the corresponding frequency distributions of TOC percentage differences (Delta–Brewer), with mean, median, and percentile ranges indicated.

Figure 9 shows the comparison of TOC measurements of Delta (VIS shown on top panel and UV on the bottom panel) with the collocated Pandora system. The number of collocations in this case is higher than in the Delta-Brewer comparison, since Pandora has a significantly higher sampling rate than the Brewer. Both products show very good consistency with Pandora, with R^2 values exceeding 0.98. The VIS retrievals (panel a) exhibit a slope of 0.966 and a small negative bias (mean and median of –0.49% and –0.63%, respectively), while the UV retrievals (panel b) yield a slope slightly above unity (1.016) and biases closer to zero (mean and median of –0.27% and –0.32%, respectively). These differences remain well within the typical uncertainty range of ground-based TOC retrievals. The frequency distributions confirm that most of the differences are confined to a narrow ±2% range, with interquartile ranges of about 1%. The Delta–Pandora agreement is similar to the Brewer comparison, but with a slightly negative bias in the VIS. Overall, the intercomparison results indicate that both the UV and VIS retrievals of Delta are in very good agreement with the Brewer and Pandora, with only minimal systematic deviations of less than ±0.5%. This confirms that the VIS retrievals can achieve performance levels comparable to the established UV-based measurements, supporting the feasibility of exploiting the Chappuis bands for TOC retrievals from DS observations.

https://doi.org/10.5194/egusphere-2025-5627
Preprint. Discussion started: 5 January 2026

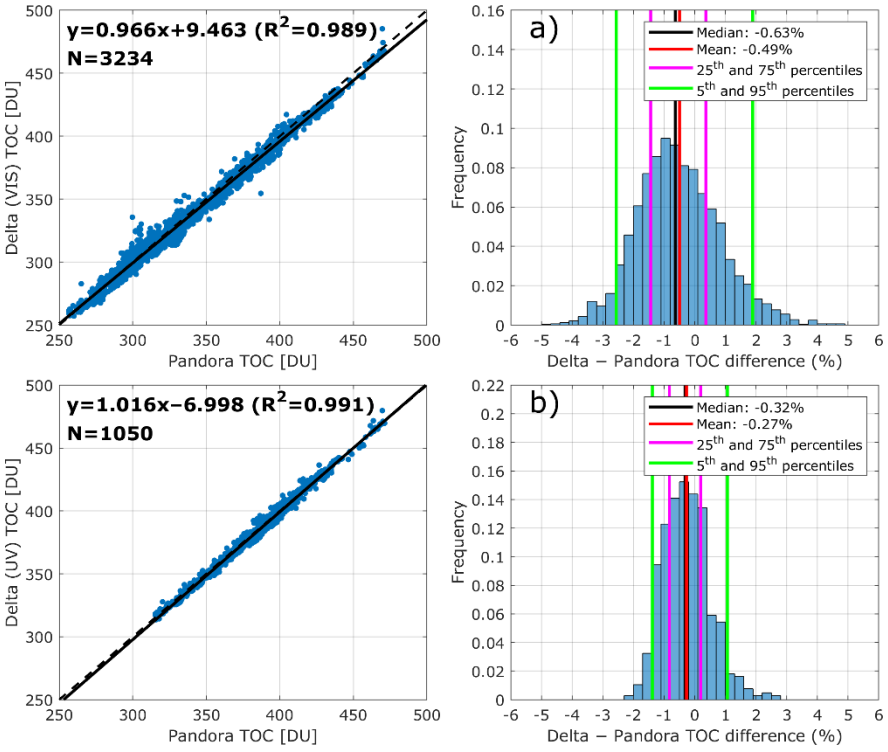

Figure 9: Same as Figure 8 but for the comparison of TOC measurements of Delta with Pandora.

The time series of the TOC percentage differences between Delta VIS and Brewer (panel a) and between Delta VIS and Pandora (panel b) over the whole period of study is shown in Figure 10. No corresponding time series are shown for the UV retrievals, since the available six-month record is not long enough to allow for a meaningful assessment of the seasonal behavior. Individual collocated measurements are shown in black, while blue markers represent daily means.

The temporal patterns of the respective percentage differences against Brewer and Pandora are very similar, showing a weak seasonal variability, with slightly positive deviations during summer and slightly negative ones in winter, likely related to the seasonal variation of SZA and to the seasonality of the AOD in Thessaloniki, as discussed in Sect. 4.4., Nevertheless, the overall performance of the VIS retrievals remains stable throughout the year. In both cases, most differences lie within ±3%, with a few outliers. The largest deviations, reaching up to ~12%, occurred on 23 August 2023, coinciding with an extreme wildfire event that took place close to the city of Alexandroupolis, Greece, at a distance of approximately 250 km east of Thessaloniki (Michailidis et al., 2024; Koukouli et al., 2025). The smoke plume was transported over Thessaloniki and was detected at LAP.AUTH between the 22nd and 25th of August, resulting in record high Aerosol Optical Depth (AOD), reaching values up to 3.35 at 340 nm and at 2.39 at 500 nm, and reduction of surface solar UV irradiance by up to 90%. High aerosol load with elevated AOD in April–May 2024 also contributed to enhanced TOC differences, though of smaller magnitude (up to 7%). The effect of aerosols on the retrieved TOC is further discussed in Sect. 4.4.

https://doi.org/10.5194/egusphere-2025-5627
Preprint. Discussion started: 5 January 2026

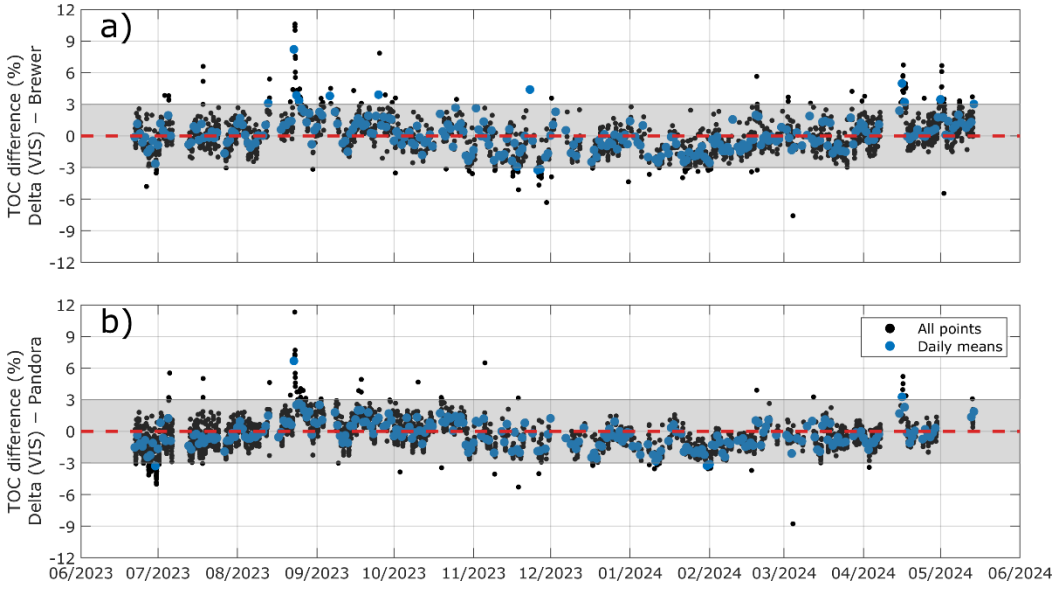

Figure 10: Time series of relative TOC differences between Delta (VIS) and Brewer (a) and Delta (VIS) and Pandora (b). Black markers represent all collocated measurements, while blue markers show daily mean differences. The shaded grey area corresponds to the ±3% range around zero (red dashed line)

The dependence of TOC percentage differences on SZA, separated by season, is shown in Figure 11. Panels (a) and (b) show the differences of Delta VIS and UV retrievals with the Brewer, while panels (c) and (d) show the differences with Pandora, respectively. It should be noted that the Brewer observations are not continuous in time, since the instrument follows a fixed operational schedule and performs measurements at specific SZAs. In contrast, Delta and Pandora provide quasi-continuous direct-sun measurements throughout the day, which explains the denser temporal coverage of these datasets. In the UV retrievals (panels b and d), the differences show a narrow distribution with minimal scatter, in line with the intercomparison results presented in Figure 8 and Figure 9. As already discussed, TOC data are available from the Delta UV channel only in winter and spring. Especially in the comparison with Pandora (panel d), the differences are distributed very smoothly for SZAs below 70°, with most points lying within ±3% and without clear seasonal dependence. At higher SZAs (>70°), a positive drift is found, possibly reflecting the increasing influence of straylight. This effect is most pronounced in the comparison with the Brewer, which being a single-monochromator instrument suffers by straylight, leading to underestimation of TOC at large SZAs (e.g., Redondas et al., 2018). Delta is also impacted by straylight, though to a lesser degree, which explains the smaller drift in the Delta–Pandora comparison.

The VIS retrievals (panels a and c) show a much larger scatter across the entire SZA range, which is consistent with the intercomparison results. Any systematic effect, such as the drift observed in the UV, is likely masked by the larger spread. In the Delta VIS–Pandora comparison (panel c) a negative drift is found during summer at low SZAs, which is not observed in the corresponding Brewer comparison, for reasons not yet identified. We also tested the non-operational Pandora v1.9.7 ozone dataset, which employs a fitted effective ozone temperature and includes a stray-light correction compared to the operational v1.8.49 that is currently used, but no major differences were found. Nevertheless, no clear seasonal dependence is found in

https://doi.org/10.5194/egusphere-2025-5627
Preprint. Discussion started: 5 January 2026

either spectral range, and overall, the results indicate that the VIS retrievals provide consistent performance despite their larger scatter, while UV retrievals show less variable comparisons both with the Brewer and the Pandora, but require careful consideration of straylight effects at large SZAs.

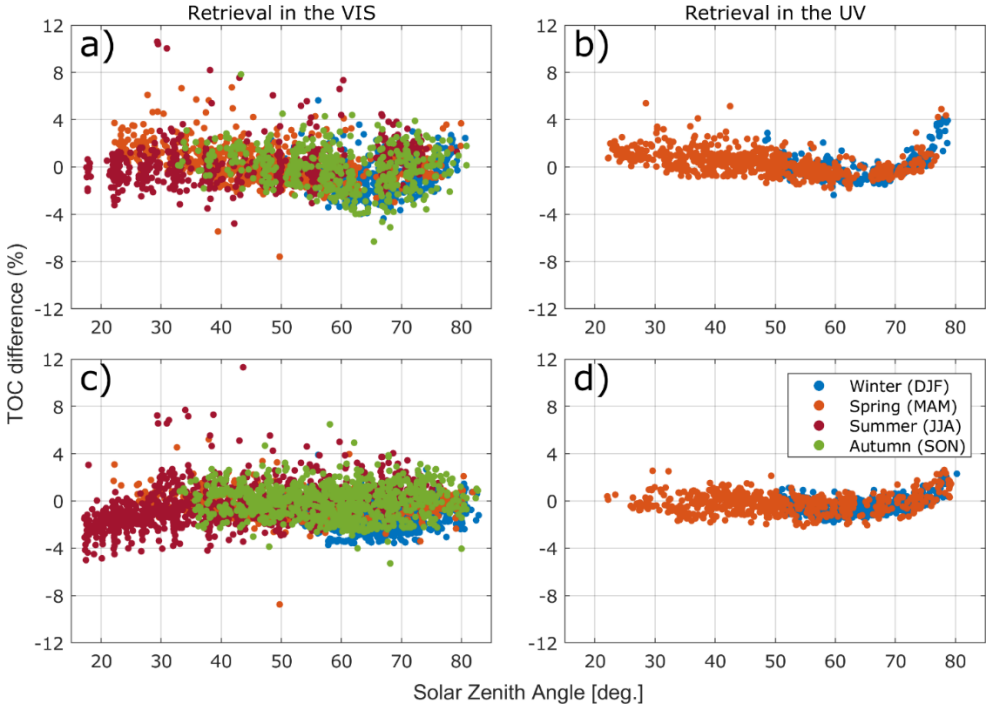

Figure 11: Seasonal dependence of TOC differences between Delta-Brewer, and Delta-Pandora as a function of SZA. The top row shows the percentage differences of Delta VIS (a) and Delta UV (b) with the Brewer, while the bottom row shows the corresponding differences with the Pandora (c and d).

4.3 Temporal variability

The seasonal cycle of monthly mean TOC measured by Delta, Brewer, and Pandora between June 2023 and May 2024 is presented in Figure 12. All three instruments capture a very similar annual variability, with TOC values decreasing from early summer to autumn, reaching their minimum in October (~290 DU), and subsequently increasing through winter to peak in spring (~400 DU in April–May). This behavior is fully consistent with the well-documented seasonal ozone cycle over Thessaloniki (e.g., Zerefos et al., 1998, 2000; Fragkos et al., 2016; Garane et al., 2024). The agreement among the three datasets is very good throughout the entire period, with the individual monthly mean data almost overlapping, being well within ±3% of the Brewer TOC data (shaded area). Brewer and Pandora are in almost excellent agreement, while Delta shows slightly lower values from October until December, coinciding with the seasonal minimum, and slightly higher values during the late spring maximum. However, these differences remain small compared to the expected uncertainty range and do not affect the overall consistency of the seasonal variability.

https://doi.org/10.5194/egusphere-2025-5627
Preprint. Discussion started: 5 January 2026

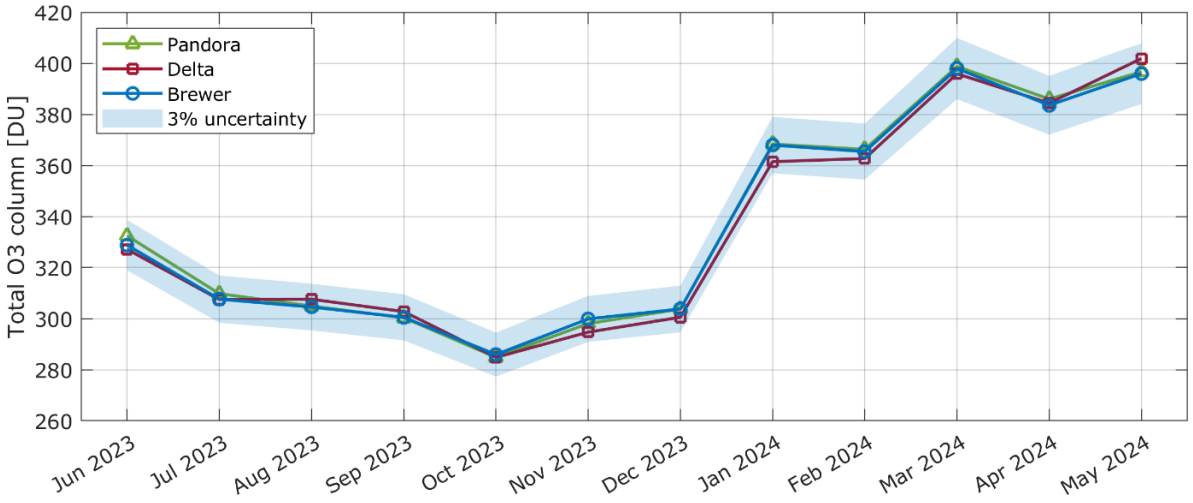

Figure 12: The seasonal variability of TOC captured by Pandora (green), Delta VIS (red), and Brewer (blue). The shaded blue area represents the ±3% uncertainty range around the Brewer observations.

As a next step, the agreement of the three datasets in terms of the TOC diurnal variability was investigated. Examples are shown in Figure 13 for selected days under cloud-free conditions, that were specifically chosen due to interesting features in their diurnal cycle. Delta UV retrievals were not yet operational in 2023 and thus the respective data are missing from the top row of figures. For most days, all three instruments follow a very consistent evolution throughout the day, with only small deviations and no systematic biases. A notable exception is observed on 31 August 2023, where in the morning hours all instruments are in very good agreement, but in the afternoon the Delta VIS retrievals begin to overestimate TOC compared to Brewer and Pandora. This divergence coincides with a substantial increase in AOD (from less than 0.2 to ~0.9 at 500 nm), as recorded by the collocated CIMEL sun-photometer, pointing to enhanced aerosol load as the primary driver of the discrepancy. The sensitivity of Delta VIS retrievals to high aerosol loads is also consistent with the findings from the Alexandroupolis wildfire case (Supplement Sect. S3). Figure S3 illustrates this case in detail, showing the diurnal evolution of TOC from Delta VIS, Brewer, and Pandora between 20 and 24 August 2023 (top panels), along with collocated AOD observations at 340 and 500 nm from the CIMEL sun-photometer (bottom panels). During the first two days of the event (20 and 21 August), the agreement among all instruments is very good throughout the day, with TOC differences generally remaining within the expected ±3% uncertainty range. AOD is low (<0.5), indicating relatively clean conditions and is associated with negligible aerosol influence on the TOC retrievals. From 22 August onward, however, the influence of wildfire smoke becomes evident. AOD increases sharply, peaking at values over 3 at 340 nm on 23 August. On this day, Delta VIS shows a clear positive bias compared to the reference instruments, while even Brewer and Pandora, which typically agree closely, exhibit noticeable differences. On 24 August, AOD values remain elevated (AOD>1 at 340 nm) but lower than in the previous day. TOC differences are still evident, with Delta VIS maintaining a positive bias relative to Brewer and Pandora, though less pronounced than during the peak of the event. The broader statistical picture of the TOC diurnal variability captured is provided in Figure S4 (Supplement Sect. S4), which shows boxplots of TOC values for Delta VIS (top) and Delta UV (bottom) compared with

https://doi.org/10.5194/egusphere-2025-5627
Preprint. Discussion started: 5 January 2026

collocated Brewer and Pandora observations. The variability of all three instruments' distribution is higher in the top panel since the VIS dataset covers an 11-month period, whereas the UV dataset spans only 6 months, resulting in a narrower statistical spread. At very early or late hours of the day, when SZAs are high, the number of available measurements is smaller, which can explain the different behavior of the distributions in those time bins. In both spectral ranges, the three instruments show a high degree of consistency across the day, with median values closely aligned and interquartile ranges overlapping and overall, no systematic diurnal drift is apparent in either case.

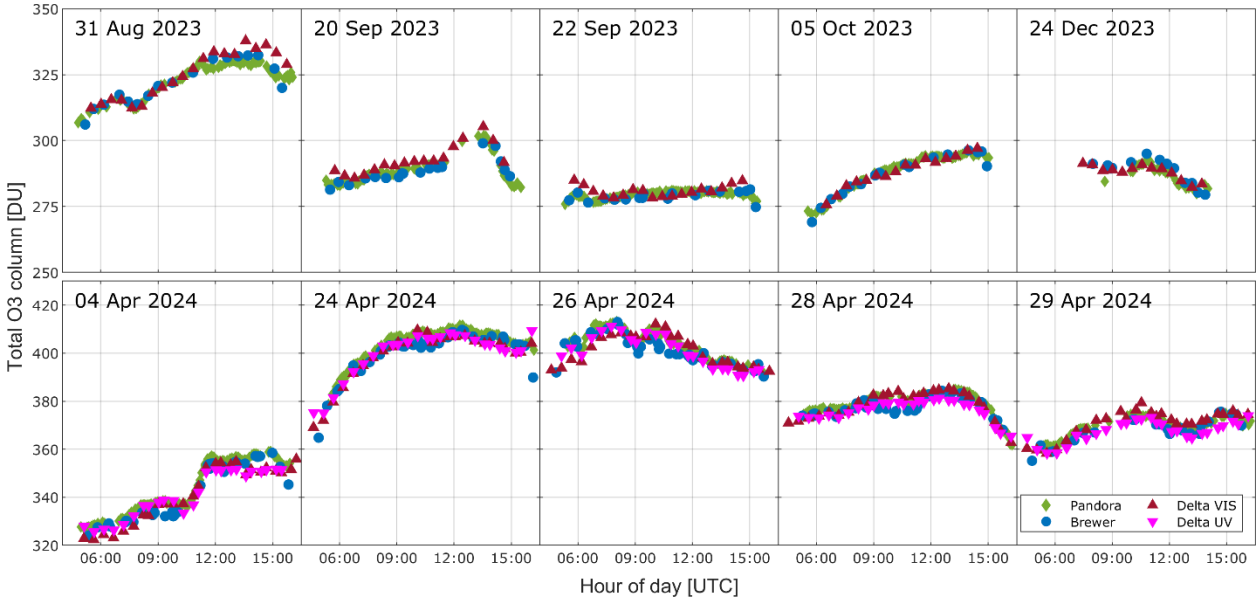

Figure 13: The diurnal variability of TOC captured by Pandora (green), Brewer (blue), Delta VIS (red) and Delta UV (magenta) for selected days.

4.4 Dependency of TOC retrieval on AOD

Figure 14 shows the TOC differences of Delta VIS (panel a) and Delta UV (panel b) from Pandora and Brewer as a function of AOD at 500 nm. We used Level 1.5 data from the collocated Aerosol Robotic Network (AERONET) station, which represent near-real-time, automatically cloud-screened observations, because Level 2 data were not yet available for the entire period. A temporal collocation criterion of ±10 minutes was applied, the same that was used in the intercomparison of Delta with Brewer and Pandora TOC measurements. In the VIS retrievals (panel a), a clear positive dependence of TOC differences with AOD is found with R=0.57 and R=0.62 for Pandora and Brewer, respectively. This suggests that under high AOD conditions, the VIS retrievals of Delta tend to overestimate TOC compared to both reference instruments. This behavior may be related to the wavelength-dependent impact of aerosols on radiative transfer. Aerosol scattering and absorption modify the effective optical path lengths differently in the UV and visible spectral ranges and can affect AMFs, which, if not fully accounted for in the retrieval, propagate into a bias in the retrieved ozone columns. However, investigation of this effect with RTM simulations is beyond the scope of this study.

https://doi.org/10.5194/egusphere-2025-5627
Preprint. Discussion started: 5 January 2026

The sensitivity of VIS retrievals to aerosol contamination is consistent with the diurnal patterns identified in Supplement Sect. S3, where episodes of elevated AOD, such as during the Alexandroupolis wildfire event, were associated with enhanced discrepancies. In contrast, the Delta UV retrievals (panel b) exhibit almost no dependence on AOD (R=0.03 and R=0.09 with the Pandora and the Brewer, respectively), indicating that the effect of aerosols is negligible in this spectral region. This might be expected since for all three instruments TOC is retrieved from radiances in the UV, hence aerosol-related path length modifications are similar and are effectively cancelled out in the comparisons. In addition, we investigated the dependency of the differences between Delta (VIS) and Delta (UV) TOC retrievals on the AOD, which resulted in a less pronounced correlation coefficient (R=0.25). It should be noted, however, that the UV dataset does not cover summer months, when AOD in Thessaloniki typically reaches its highest values (Kazadzis et al., 2007; Siomos et al., 2018; Fountoulakis et al., 2019a), and therefore the statistical robustness is limited.

The contrast between the TOC retrievals in the two spectral ranges highlights that aerosol effects should be considered in VIS-based TOC retrievals. In particular, it demonstrates the need for AMFs that explicitly incorporate both the spectral dependence of ozone absorption and the influence of aerosols on the effective optical path. In this study, the DS AMF applied for both UV and VIS retrievals is solely based on a geometrical approximation according to Eq. (4), a similar approach that is also applied operationally to Brewer and Pandora instruments, without accounting for aerosol effects. Such corrections would potentially reduce the observed discrepances and help bring VIS retrievals closer to the UV retrievals, which appear more robust under varying aerosol conditions. However, to confirm this, further investigation is required, which is beyond the scope of this study.

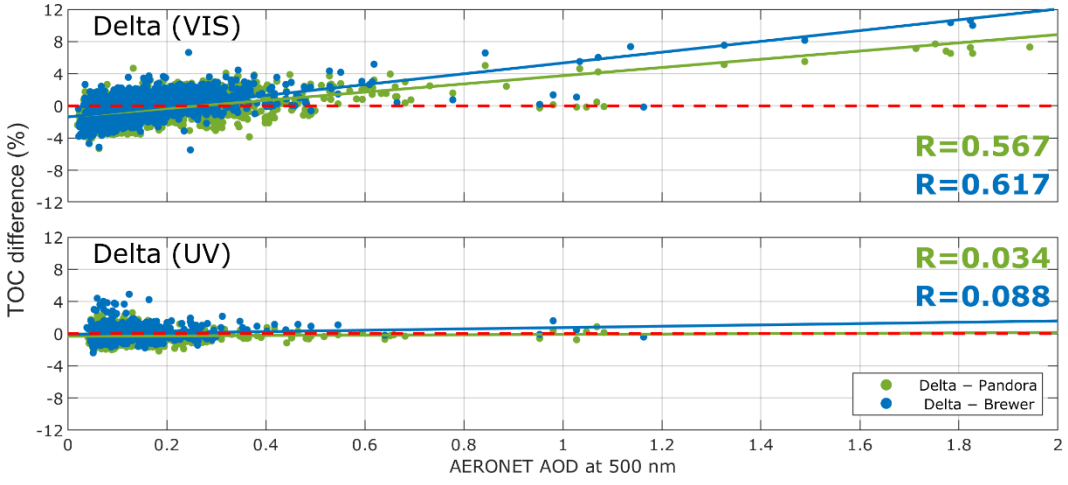

Figure 14: TOC differences of Delta from Pandora (green markers) and Brewer (blue markers) retrieved in the VIS (top panel) and the UV (bottom panel) spectral ranges as a function of AOD at 500 nm.

5 Summary and Conclusions

In this study, total ozone column retrievals were performed in both Huggins and Chappuis bands using direct-sun DOAS observations from the recently developed Delta UV–VIS system in Thessaloniki. By applying a dedicated retrieval algorithm and appropriate calibration procedures, reliable TOC measurements were obtained across both spectral regions. The analysis

https://doi.org/10.5194/egusphere-2025-5627
Preprint. Discussion started: 5 January 2026

indicated very good internal consistency between UV- and VIS-based retrievals, with differences typically below 2%. This confirms that ozone absorption in the Chappuis bands, although weaker than in the Huggins bands, can be successfully exploited to derive TOC of comparable quality to those obtained in the UV. Comparisons with collocated Brewer and Pandora instruments further validate the robustness of the Delta measurements. In both spectral regions, the agreement with the two reference instruments is very good, with correlation coefficients (R) exceeding 0.98. The median biases of the Delta VIS TOC retrievals from the Brewer and Pandora are –0.18% and –0.63%, respectively, and 0.08% and –0.32% for Delta UV. The VIS retrievals show slightly larger scatter and a subtle negative bias compared to the UV, but their overall performance remain well within the uncertainty range of direct-sun TOC observations. Seasonal and diurnal cycles, as well as the interannual variability of TOC over Thessaloniki, are consistently captured by all three instruments, showing coherent temporal patterns and good agreement between the different datasets.

The analysis indicates that the differences between TOC retrievals in the VIS from Delta and the reference instruments exhibit a dependence on aerosol load, likely due to the wavelength-dependent effects of aerosol scattering and absorption on effective optical path lengths. Increased aerosol loads, such as during the Alexandroupolis wildfire event in August 2023, resulted in significant positive deviations in the VIS TOC comparisons with the reference instruments, whereas in the UV, the differences remained comparatively small. This finding highlights the importance of accounting for aerosol effects in future refinements of the VIS retrieval approach, including the development of AMFs that consider the impact of aerosol scattering and absorption across different domains of the spectrum. Moreover, since TOC retrievals in the Chappuis bands require higher signal-to-noise ratios than the Huggins bands, further investigation is needed to assess their applicability across a wider range of ground-based DOAS instruments, especially those with lower sensitivity or different optical characteristics.

Future work is expected to improve the statistical robustness of these results as the time series are expanded with additional years of observations. Furthermore, the use of a synthetic, absorption-free reference spectrum in the TOC retrieval algorithm, instead of a measured FRS, could be investigated to determine whether it improves the effectiveness of the approach. In that case the measured reference spectrum would not require calibration for determining its O_3 SCD. However, the current results suggest that the Delta instrument provides reliable TOC retrievals in both UV and VIS ranges of acceptable quality, demonstrating the feasibility of employing the Chappuis bands as a complementary approach to the traditional Huggins band retrievals of TOC. This capability broadens the applicability of DOAS-based ozone monitoring, particularly under conditions where UV sensitivity is limited, such as at high latitudes or high SZAs. The successful intercomparison with Brewer and Pandora also establishes a strong framework for the continued integration of Delta measurements into long-term monitoring and satellite validation activities.

Acknowledgments

This work was carried out in the frame of the Instrument Data quality Evaluation and Assessment Service - Quality Assurance for Earth Observation (IDEAS-QA4EO) contract funded by ESA-ESRIN (n. 4000128960/19/I-NS) and builds on the work of previous projects. The authors would like to warmly thank Caroline Fayt (caroline.fayt@aeronomie.be) and Thomas Danckaert

https://doi.org/10.5194/egusphere-2025-5627
Preprint. Discussion started: 5 January 2026

(thomas.danckaert@aeronomie.be) from the Royal Belgian Institute for Space Aeronomy (BIRA-IASB) for the free use of the QDOAS software. We also thank PGN, a bilateral project supported with funding from NASA and ESA.

Financial support

This research received funding by the European Space Agency's FRM Programme under grant agreement 4000135355/21/I-DT-Ir (FRM4DOAS-2.0). The research has also been supported by the project "Panhellenic infrastructure for Atmospheric Composition and Climate change" (MIS 5021516), which is implemented under the Action "Reinforcement of the Research and Innovation Infrastructure", funded by the Operational Programme "Competitiveness, Entrepreneurship and Innovation" (NSRF 2014-2020) and co-financed by Greece and the European Union (European Regional Development Fund).

Data availability

Total Ozone Column data from the Delta instrument that were analyzed during the current study are available upon request from D. Karagkiozidis (dkaragki@auth.gr) or A.F. Bais (abais@auth.gr). Data from the Brewer spectrophotometer are available from WOUDC (https://woudc.org/en/, last access: 8 November 2025) as well as also available upon request from A.F. Bais or K. Garane (agarane@auth.gr). The Pandora 240 operational L2 data from Thessaloniki are publicly available from the official PGN website (https://data.hetzner.pandonia-global-network.org/Thessaloniki/Pandora240s1/L2/, last access: 8 November 2025).

Author contributions

DK performed the retrievals of TOC for Delta in the UV and VIS ranges, developed the intercomparison strategy, conducted the data analysis from Delta, Pandora, Brewer and CIMEL instruments, and wrote the manuscript. KG provided the TOC data from the Brewer spectrophotometer. MVR, MR and DN reviewed the paper. AB supervised the whole study and provided general guidance for the manuscript preparation. All authors discussed, commented on, and helped review the manuscript.

Competing interests

At least one of the (co-)authors is a member of the editorial board of Atmospheric Measurement Techniques.

References

Amiridis, V., Kazadzis, S., Gkikas, A., Voudouri, K. A., Kouklaki, D., Koukouli, M.-E., Garane, K., Georgoulias, A. K., Solomos, S., Varlas, G., Kampouri, A., Founda, D., Psiloglou, B. E., Katsafados, P., Papachristopoulou, K., Fountoulakis, I., Raptis, P.-I., Georgiou, T., Gialitaki, A., Proestakis, E., Tsekeri, A., Drakaki, E., Marinou, E., Giannakaki, E., Misios, S., Kapsomenakis, J., Eleftheratos, K., Hatzianastassiou, N., Kalabokas, P., Zanis, P., Vrekoussis, M., Papayannis, A., Kazantzidis, A., Kourtidis, K., Balis, D., Bais, A. F., and Zerefos, C.: Natural Aerosols, Gaseous Precursors and Their Impacts

https://doi.org/10.5194/egusphere-2025-5627
Preprint. Discussion started: 5 January 2026

in Greece: A Review from the Remote Sensing Perspective, Atmosphere, 15, 753, https://doi.org/10.3390/atmos15070753, 2024.

Bais, A. F., Zerefos, C. S., Meleti, C., Ziomas, I. C., and Tourpali, K.: Spectral measurements of solar UVB radiation and its relations to total ozone, SO2, and clouds, Journal of Geophysical Research: Atmospheres, 98, 5199–5204, https://doi.org/10.1029/92JD02904, 1993.

Bass, A. M. and Paur, R. J.: The Ultraviolet Cross-Sections of Ozone: I. The Measurements, in: Atmospheric Ozone, edited by: Zerefos, C. S. and Ghazi, A., Springer Netherlands, Dordrecht, 606–610, https://doi.org/10.1007/978-94-009-5313-0_120, 1985.

Brewer, A. W.: A replacement for the Dobson spectrophotometer?, PAGEOPH, 106–108, 919–927, https://doi.org/10.1007/BF00881042, 1973.

Cede, A., Herman, J., Richter, A., Krotkov, N., and Burrows, J.: Measurements of nitrogen dioxide total column amounts using a Brewer double spectrophotometer in direct Sun mode, Journal of Geophysical Research: Atmospheres, 111, https://doi.org/10.1029/2005JD006585, 2006.

Chance, K. and Kurucz, R. L.: An improved high-resolution solar reference spectrum for earth's atmosphere measurements in the ultraviolet, visible, and near infrared, Journal of Quantitative Spectroscopy and Radiative Transfer, 111, 1289–1295, https://doi.org/10.1016/j.jqsrt.2010.01.036, 2010.

Chubachi, S.: A Special Ozone Observation at Syowa Station, Antarctica from February 1982 to January 1983, in: Atmospheric Ozone, edited by: Zerefos, C. S. and Ghazi, A., Springer Netherlands, Dordrecht, 285–289, https://doi.org/10.1007/978-94-009-5313-0_58, 1985.

Crutzen, P. J.: The Role of NO and NO2 in the Chemistry of the Troposphere and Stratosphere, Annual Review of Earth and Planetary Sciences, 7, 443–472, https://doi.org/10.1146/annurev.ea.07.050179.002303, 1979.

Dobson, G. M. B.: A photoelectric spectrophotometer for measuring the amount of atmospheric ozone, Proc. Phys. Soc., 43, 324–339, https://doi.org/10.1088/0959-5309/43/3/308, 1931.

Donner, S., Kuhn, J., Van Roozendael, M., Bais, A., Beirle, S., Bösch, T., Bognar, K., Bruchkouski, I., Chan, K. L., Dörner, S., Drosoglou, T., Fayt, C., Frieß, U., Hendrick, F., Hermans, C., Jin, J., Li, A., Ma, J., Peters, E., Pinardi, G., Richter, A., Schreier, S. F., Seyler, A., Strong, K., Tirpitz, J.-L., Wang, Y., Xie, P., Xu, J., Zhao, X., and Wagner, T.: Evaluating different methods for elevation calibration of MAX-DOAS (Multi AXis Differential Optical Absorption Spectroscopy) instruments during the CINDI-2 campaign, Atmos. Meas. Tech., 13, 685–712, https://doi.org/10.5194/amt-13-685-2020, 2020.

Farman, J. C., Gardiner, B. G., and Shanklin, J. D.: Large losses of total ozone in Antarctica reveal seasonal ClOx/NOx interaction, Nature, 315, 207–210, https://doi.org/10.1038/315207a0, 1985.

Fioletov, V. E., Bodeker, G. E., Miller, A. J., McPeters, R. D., and Stolarski, R.: Global and zonal total ozone variations estimated from ground-based and satellite measurements: 1964–2000, J.-Geophys.-Res., 107, https://doi.org/10.1029/2001JD001350, 2002.

https://doi.org/10.5194/egusphere-2025-5627
Preprint. Discussion started: 5 January 2026

Fountoulakis, I., Natsis, A., Siomos, N., Drosoglou, T., and Bais, A. F.: Deriving Aerosol Absorption Properties from Solar Ultraviolet Radiation Spectral Measurements at Thessaloniki, Greece, Remote Sensing, 11, https://doi.org/10.3390/rs11182179, 2019a.

Fountoulakis, I., Diémoz, H., Siani, A.-M., Laschewski, G., Filippa, G., Arola, A., Bais, A. F., De Backer, H., Lakkala, K., Webb, A. R., De Bock, V., Karppinen, T., Garane, K., Kapsomenakis, J., Koukouli, M.-E., and Zerefos, C. S.: Solar UV Irradiance in a Changing Climate: Trends in Europe and the Significance of Spectral Monitoring in Italy, Environments, 7, 1, https://doi.org/10.3390/environments7010001, 2019b.

Fowler, D., Pilegaard, K., Sutton, M. A., Ambus, P., Raivonen, M., Duyzer, J., Simpson, D., Fagerli, H., Fuzzi, S., Schjoerring, J. K., Granier, C., Neftel, A., Isaksen, I. S. A., Laj, P., Maione, M., Monks, P. S., Burkhardt, J., Daemmgen, U., Neirynck, J., Personne, E., Wichink-Kruit, R., Butterbach-Bahl, K., Flechard, C., Tuovinen, J. P., Coyle, M., Gerosa, G., Loubet, B., Altimir, N., Gruenhage, L., Ammann, C., Cieslik, S., Paoletti, E., Mikkelsen, T. N., Ro-Poulsen, H., Cellier, P., Cape, J. N., Horváth, L., Loreto, F., Niinemets, Ü., Palmer, P. I., Rinne, J., Misztal, P., Nemitz, E., Nilsson, D., Pryor, S., Gallagher, M. W., Vesala, T., Skiba, U., Brüggemann, N., Zechmeister-Boltenstern, S., Williams, J., O'Dowd, C., Facchini, M. C., de Leeuw, G., Flossman, A., Chaumerliac, N., and Erisman, J. W.: Atmospheric composition change: Ecosystems–Atmosphere interactions, Atmospheric Environment, 43, 5193–5267, https://doi.org/10.1016/j.atmosenv.2009.07.068, 2009.

Fragkos, K., Bais, A. F., Balis, D., Meleti, C., and Koukouli, M. E.: The Effect of Three Different Absorption Cross-Sections and their Temperature Dependence on Total Ozone Measured by a Mid-Latitude Brewer Spectrophotometer, Atmosphere-Ocean, 53, 19–28, https://doi.org/10.1080/07055900.2013.847816, 2015.

Fragkos, K., Bais, A. F., Fountoulakis, I., Balis, D., Tourpali, K., Meleti, C., and Zanis, P.: Extreme total column ozone events and effects on UV solar radiation at Thessaloniki, Greece, Theor Appl Climatol, 126, 505–517, https://doi.org/10.1007/s00704-015-1562-3, 2016.

Garane, K., Fountoulakis, I., Karanikolas, A., Bais, A. F., and Meleti, C.: Thirty years of solar ultraviolet spectral irradiance measurements in Thessaloniki: Variability and trends, Radiation Processes In The Atmosphere And Ocean, Thessaloniki, Greece, AIP Conf. Proc. 18 January 2024; 2988 (1): 090003, https://doi.org/10.1063/5.0183293, 2024.

Gkertsi, F., Bais, A. F., Kouremeti, N., Drosoglou, T., Fountoulakis, I., and Fragkos, K.: DOAS-based total column ozone retrieval from Phaethon system, Atmospheric Environment, 180, 51–58, https://doi.org/10.1016/j.atmosenv.2018.02.036, 2018.

Gröbner, J. and Kerr, J. B.: Ground-based determination of the spectral ultraviolet extraterrestrial solar irradiance: Providing a link between space-based and ground-based solar UV measurements, J. Geophys. Res., 106, 7211–7217, https://doi.org/10.1029/2000JD900756, 2001.

Gröbner, J. and Meleti, C.: Aerosol optical depth in the UVB and visible wavelength range from Brewer spectrophotometer direct irradiance measurements: 1991–2002, Journal of Geophysical Research: Atmospheres, 109, https://doi.org/10.1029/2003JD004409, 2004.

https://doi.org/10.5194/egusphere-2025-5627
Preprint. Discussion started: 5 January 2026

Gröbner, J., Schill, H., Egli, L., and Stübi, R.: Consistency of total column ozone measurements between the Brewer and Dobson spectroradiometers of the LKO Arosa and PMOD/WRC Davos, Atmos. Meas. Tech., 14, 3319–3331, https://doi.org/10.5194/amt-14-3319-2021, 2021.

Harris, N. R. P., Ancellet, G., Bishop, L., Hofmann, D. J., Kerr, J. B., McPeters, R. D., Prendez, M., Randel, W. J., Staehelin, J., Subbaraya, B. H., Volz-Thomas, A., Zawodny, J., and Zerefos, C. S.: Trends in stratospheric and free tropospheric ozone, J. Geophys. Res., 102, 1571–1590, https://doi.org/10.1029/96JD02440, 1997.

Hendrick, F., Pommereau, J.-P., Goutail, F., Evans, R. D., Ionov, D., Pazmino, A., Kyrö, E., Held, G., Eriksen, P., Dorokhov, V., Gil, M., and Van Roozendael, M.: NDACC/SAOZ UV-visible total ozone measurements: improved retrieval and comparison with correlative ground-based and satellite observations, Atmospheric Chemistry and Physics, 11, 5975–5995, https://doi.org/10.5194/acp-11-5975-2011, 2011.

Herman, J., Cede, A., Spinei, E., Mount, G., Tzortziou, M., and Abuhassan, N.: NO2 column amounts from ground-based Pandora and MFDOAS spectrometers using the direct-sun DOAS technique: Intercomparisons and application to OMI validation, Journal of Geophysical Research: Atmospheres, 114, https://doi.org/10.1029/2009JD011848, 2009.

Herman, J., Evans, R., Cede, A., Abuhassan, N., Petropavlovskikh, I., and McConville, G.: Comparison of ozone retrievals from the Pandora spectrometer system and Dobson spectrophotometer in Boulder, Colorado, Atmospheric Measurement Techniques, 8, 3407–3418, https://doi.org/10.5194/amt-8-3407-2015, 2015.

Hönninger, G., von Friedeburg, C., and Platt, U.: Multi axis differential optical absorption spectroscopy (MAX-DOAS), Atmospheric Chemistry and Physics, 4, 231–254, https://doi.org/10.5194/acp-4-231-2004, 2004.

Judd, L. M., Al-Saadi, J. A., Szykman, J. J., Valin, L. C., Janz, S. J., Kowalewski, M. G., Eskes, H. J., Veefkind, J. P., Cede, A., Mueller, M., Gebetsberger, M., Swap, R., Pierce, R. B., Nowlan, C. R., Abad, G. G., Nehrir, A., and Williams, D.: Evaluating Sentinel-5P TROPOMI tropospheric NO_2 column densities with airborne and Pandora spectrometers near New York City and Long Island Sound, Atmos. Meas. Tech., 13, 6113–6140, https://doi.org/10.5194/amt-13-6113-2020, 2020.

Karagkiozidis, D.: Remote sensing of the vertical distribution of gaseous pollutants and aerosols in the troposphere by differential optical absorption spectroscopy and comparison with satellite observations, https://doi.org/10.26262/HEAL.AUTH.IR.351247, 2023.

Kazadzis, S., Bais, A., Amiridis, V., Balis, D., Meleti, C., Kouremeti, N., Zerefos, C. S., Rapsomanikis, S., Petrakakis, M., Kelesis, A., Tzoumaka, P., and Kelektsoglou, K.: Nine years of UV aerosol optical depth measurements at Thessaloniki, Greece, Atmospheric Chemistry and Physics, 7, 2091–2101, https://doi.org/10.5194/acp-7-2091-2007, 2007.

Kerr, J. B., McElroy, C. T., and Olafson, R. A.: Measurements of ozone with the Brewer ozone spectrophotometer, in: Quadrennial International Ozone Symposium, Boulder, CO, edited by J. London, vol. I, pp. 74–79, Natl. Cent. for Atmos. Res, 1981.

Kerr, J. B., Asbridge, I. A., and Evans, W. F. J.: Intercomparison of total ozone measured by the Brewer and Dobson spectrophotometers at Toronto, J. Geophys. Res., 93, 11129–11140, https://doi.org/10.1029/JD093iD09p11129, 1988.

https://doi.org/10.5194/egusphere-2025-5627
Preprint. Discussion started: 5 January 2026

Kim, J., Kim, J., Cho, H.-K., Herman, J., Park, S. S., Lim, H. K., Kim, J.-H., Miyagawa, K., and Lee, Y. G.: Intercomparison of total column ozone data from the Pandora spectrophotometer with Dobson, Brewer, and OMI measurements over Seoul, Korea, Atmospheric Measurement Techniques, 10, 3661–3676, https://doi.org/10.5194/amt-10-3661-2017, 2017.

Koukouli, M.-E., Pseftogkas, A., Karagkiozidis, D., Mermigkas, M., Panou, T., Balis, D., and Bais, A.: Extreme wildfires over Northern Greece during Summer 2023 – Part B. Adverse effects on regional air quality, Atmospheric Research, 320, https://doi.org/10.1016/j.atmosres.2025.108034, 2025.

Kreher, K., Van Roozendael, M., Hendrick, F., Apituley, A., Dimitropoulou, E., Frieß, U., Richter, A., Wagner, T., Lampel, J., Abuhassan, N., Ang, L., Anguas, M., Bais, A., Benavent, N., Bösch, T., Bognar, K., Borovski, A., Bruchkouski, I., Cede, A., Chan, K. L., Donner, S., Drosoglou, T., Fayt, C., Finkenzeller, H., Garcia-Nieto, D., Gielen, C., Gómez-Martín, L., Hao, N., Henzing, B., Herman, J. R., Hermans, C., Hoque, S., Irie, H., Jin, J., Johnston, P., Khayyam Butt, J., Khokhar, F., Koenig, T. K., Kuhn, J., Kumar, V., Liu, C., Ma, J., Merlaud, A., Mishra, A. K., Müller, M., Navarro-Comas, M., Ostendorf, M., Pazmino, A., Peters, E., Pinardi, G., Pinharanda, M., Piters, A., Platt, U., Postylyakov, O., Prados-Roman, C., Puentedura, O., Querel, R., Saiz-Lopez, A., Schönhardt, A., Schreier, S. F., Seyler, A., Sinha, V., Spinei, E., Strong, K., Tack, F., Tian, X., Tiefengraber, M., Tirpitz, J.-L., van Gent, J., Volkamer, R., Vrekoussis, M., Wang, S., Wang, Z., Wenig, M., Wittrock, F., Xie, P. H., Xu, J., Yela, M., Zhang, C., and Zhao, X.: Intercomparison of NO_2, O_4, O_3 and HCHO slant column measurements by MAX-DOAS and zenith-sky UV–visible spectrometers during CINDI-2, Atmospheric Measurement Techniques, 13, 2169–2208, https://doi.org/10.5194/amt-13-2169-2020, 2020.

Kumar, V., Beirle, S., Dörner, S., Mishra, A. K., Donner, S., Wang, Y., Sinha, V., and Wagner, T.: Long-term MAX-DOAS measurements of NO_2, HCHO, and aerosols and evaluation of corresponding satellite data products over Mohali in the Indo-Gangetic Plain, Atmospheric Chemistry and Physics, 20, 14183–14235, https://doi.org/10.5194/acp-20-14183-2020, 2020.

Kuttippurath, J. and Nair, P. J.: The signs of Antarctic ozone hole recovery, Sci Rep, 7, 585, https://doi.org/10.1038/s41598-017-00722-7, 2017.

Langematz, U.: Stratospheric ozone: down and up through the anthropocene, ChemTexts, 5, 8, https://doi.org/10.1007/s40828-019-0082-7, 2019.

Lelieveld, J., Gromov, S., Pozzer, A., and Taraborrelli, D.: Global tropospheric hydroxyl distribution, budget and reactivity, Atmospheric Chemistry and Physics, 16, 12477–12493, https://doi.org/10.5194/acp-16-12477-2016, 2016.

Mäder, J. A., Staehelin, J., Peter, T., Brunner, D., Rieder, H. E., and Stahel, W. A.: Evidence for the effectiveness of the Montreal Protocol to protect the ozone layer, Atmos. Chem. Phys., 10, 12161–12171, https://doi.org/10.5194/acp-10-12161-2010, 2010.

Meleti, C. and Cappellani, F.: Measurements of aerosol optical depth at Ispra: Analysis of the correlation with UV-B, UV-A, and total solar irradiance, J. Geophys. Res., 105, 4971–4978, https://doi.org/10.1029/1999JD900459, 2000.

Meleti, C., Bais, A. F., Kazadzis, S., Kouremeti, N., Garane, K., and Zerefos, C.: Factors affecting solar ultraviolet irradiance measured since 1990 at Thessaloniki, Greece, International Journal of Remote Sensing, 30, 4167–4179, https://doi.org/10.1080/01431160902822864, 2009.

https://doi.org/10.5194/egusphere-2025-5627
Preprint. Discussion started: 5 January 2026

Meller, R. and Moortgat, G. K.: Temperature dependence of the absorption cross sections of formaldehyde between 223 and 323 K in the wavelength range 225–375 nm, Journal of Geophysical Research: Atmospheres, 105, 7089–7101, https://doi.org/10.1029/1999JD901074, 2000.

Michailidis, K., Garane, K., Karagkiozidis, D., Peletidou, G., Voudouri, K.-A., Balis, D., and Bais, A.: Extreme wildfires over northern Greece during summer 2023 – Part A: Effects on aerosol optical properties and solar UV radiation, Atmospheric Research, 311, 107700, https://doi.org/10.1016/j.atmosres.2024.107700, 2024.

Monks, P. S., Archibald, A. T., Colette, A., Cooper, O., Coyle, M., Derwent, R., Fowler, D., Granier, C., Law, K. S., Mills, G. E., Stevenson, D. S., Tarasova, O., Thouret, V., Von Schneidemesser, E., Sommariva, R., Wild, O., and Williams, M. L.: Tropospheric ozone and its precursors from the urban to the global scale from air quality to short-lived climate forcer, Atmos. Chem. Phys., 15, 8889–8973, https://doi.org/10.5194/acp-15-8889-2015, 2015.

Mount, G. H., Sanders, R. W., Schmeltekopf, A. L., and Solomon, S.: Visible spectroscopy at McMurdo Station, Antarctica: 1. Overview and daily variations of NO_2 and O_3 , Austral Spring, 1986, J. Geophys. Res., 92, 8320–8328, https://doi.org/10.1029/JD092iD07p08320, 1987.

Nikolis, D., Bais, A., Karagkiozidis, D., Koukouli, M.-E., and Balis, D.: Direct sun total NO2 column measurements at Thessaloniki, Greece with two DOAS systems and comparisons with S5P/TROPOMI, Atmospheric Environment, 352, https://doi.org/10.1016/j.atmosenv.2025.121161, 2025.

Noxon, J. F.: Nitrogen Dioxide in the Stratosphere and Troposphere Measured by Ground-Based Absorption Spectroscopy, Science, 189, 547–549, https://doi.org/10.1126/science.189.4202.547, 1975.

Noxon, J. F.: Stratospheric NO2: 2. Global behavior, Journal of Geophysical Research: Oceans, 84, 5067–5076, https://doi.org/10.1029/JC084iC08p05067, 1979.

Paur, R. J. and Bass, A. M.: The Ultraviolet Cross-Sections of Ozone: II. Results and Temperature Dependence, in: Atmospheric Ozone, edited by: Zerefos, C. S. and Ghazi, A., Springer Netherlands, Dordrecht, 611–616, https://doi.org/10.1007/978-94-009-5313-0_121, 1985.

Pazmiño, A., Godin-Beekmann, S., Hauchecorne, A., Claud, C., Khaykin, S., Goutail, F., Wolfram, E., Salvador, J., and Quel, E.: Multiple symptoms of total ozone recovery inside the Antarctic vortex during austral spring, Atmospheric Chemistry and Physics, 18, 7557–7572, https://doi.org/10.5194/acp-18-7557-2018, 2018.

Platt, U. and Stutz, J.: Differential optical absorption spectroscopy: principles and applications, Springer, Berlin, 2008.

Pommereau, J. P. and Goutail, F.: O_3 and NO_2 ground-based measurements by visible spectrometry during Arctic winter and spring 1988, Geophysical Research Letters, 15, 891–894, https://doi.org/10.1029/GL015i008p00891, 1988.

Puķīte, J., Kühl, S., Deutschmann, T., Platt, U., and Wagner, T.: Extending differential optical absorption spectroscopy for limb measurements in the UV, Atmos. Meas. Tech., 3, 631–653, https://doi.org/10.5194/amt-3-631-2010, 2010.

Redondas, A., Carreño, V., León-Luis, S. F., Hernández-Cruz, B., López-Solano, J., Rodriguez-Franco, J. J., Vilaplana, J. M., Gröbner, J., Rimmer, J., Bais, A. F., Savastiouk, V., Moreta, J. R., Boulkelia, L., Jepsen, N., Wilson, K. M., Shirotov, V., and

https://doi.org/10.5194/egusphere-2025-5627
Preprint. Discussion started: 5 January 2026

Karppinen, T.: EUBREWNET RBCC-E Huelva 2015 Ozone Brewer Intercomparison, Atmos. Chem. Phys., 18, 9441–9455, https://doi.org/10.5194/acp-18-9441-2018, 2018.

Robinson, J., Kotsakis, A., Santos, F., Swap, R., Knowland, K. E., Labow, G., Connors, V., Tzortziou, M., Abuhassan, N., Tiefengraber, M., and Cede, A.: Using networked Pandora observations to capture spatiotemporal changes in total column ozone associated with stratosphere-to-troposphere transport, Atmospheric Research, 238, 104872, https://doi.org/10.1016/j.atmosres.2020.104872, 2020.

Rothman, L. S., Gordon, I. E., Barber, R. J., Dothe, H., Gamache, R. R., Goldman, A., Perevalov, V. I., Tashkun, S. A., and Tennyson, J.: HITEMP, the high-temperature molecular spectroscopic database, Journal of Quantitative Spectroscopy and Radiative Transfer, 111, 2139–2150, https://doi.org/10.1016/j.jqsrt.2010.05.001, 2010.

Seinfeld, J. H. and Pandis, S. N.: Atmospheric chemistry and physics: from air pollution to climate change, Third edition., John Wiley & Sons, Inc, Hoboken, New Jersey, 1120 pp., 2016.

Serdyuchenko, A., Gorshelev, V., Weber, M., Chehade, W., and Burrows, J. P.: High spectral resolution ozone absorption cross-sections – Part 2: Temperature dependence, Atmospheric Measurement Techniques, 7, 625–636, https://doi.org/10.5194/amt-7-625-2014, 2014.

Siomos, N., Balis, D. S., Voudouri, K. A., Giannakaki, E., Filioglou, M., Amiridis, V., Papayannis, A., and Fragkos, K.: Are EARLINET and AERONET climatologies consistent? The case of Thessaloniki, Greece, Atmospheric Chemistry and Physics, 18, 11885–11903, https://doi.org/10.5194/acp-18-11885-2018, 2018.

Solomon, S., Schmeltekopf, A. L., and Sanders, R. W.: On the interpretation of zenith sky absorption measurements, Journal of Geophysical Research: Atmospheres, 92, 8311–8319, https://doi.org/10.1029/JD092iD07p08311, 1987a.

Solomon, S., Mount, G. H., Sanders, R. W., and Schmeltekopf, A. L.: Visible spectroscopy at McMurdo Station, Antarctica: 2. Observations of OClO, J. Geophys. Res., 92, 8329–8338, https://doi.org/10.1029/JD092iD07p08329, 1987b.

Solomon, S., Mount, G. H., Sanders, R. W., Jakoubek, R. O., and Schmeltekopf, A. L.: Observations of the Nighttime Abundance of OClO in the Winter Stratosphere Above Thule, Greenland, Science, 242, 550–555, https://doi.org/10.1126/science.242.4878.550, 1988.

Solomon, S., Ivy, D. J., Kinnison, D., Mills, M. J., Neely, R. R., and Schmidt, A.: Emergence of healing in the Antarctic ozone layer, Science, 353, 269–274, https://doi.org/10.1126/science.aae0061, 2016.

Spinei, E., Whitehill, A., Fried, A., Tiefengraber, M., Knepp, T. N., Herndon, S., Herman, J. R., Müller, M., Abuhassan, N., Cede, A., Richter, D., Walega, J., Crawford, J., Szykman, J., Valin, L., Williams, D. J., Long, R., Swap, R. J., Lee, Y., Nowak, N., and Poche, B.: The first evaluation of formaldehyde column observations by improved Pandora spectrometers during the KORUS-AQ field study, Atmos. Meas. Tech., 11, 4943–4961, https://doi.org/10.5194/amt-11-4943-2018, 2018.

Thalman, R. and Volkamer, R.: Temperature dependent absorption cross-sections of O2–O2 collision pairs between 340 and 630 nm and at atmospherically relevant pressure, Phys. Chem. Chem. Phys., 15, 15371–15381, https://doi.org/10.1039/C3CP50968K, 2013.

https://doi.org/10.5194/egusphere-2025-5627
Preprint. Discussion started: 5 January 2026

Tzortziou, M., Herman, J. R., Cede, A., and Abuhassan, N.: High precision, absolute total column ozone measurements from the Pandora spectrometer system: Comparisons with data from a Brewer double monochromator and Aura OMI, Journal of Geophysical Research: Atmospheres, 117, https://doi.org/10.1029/2012JD017814, 2012.

Tzortziou, M., Herman, J. R., Cede, A., Loughner, C. P., Abuhassan, N., and Naik, S.: Spatial and temporal variability of ozone and nitrogen dioxide over a major urban estuarine ecosystem, J Atmos Chem, 72, 287–309, https://doi.org/10.1007/s10874-013-9255-8, 2015.

Van Roozendael, M., Peeters, P., Roscoe, H. K., De Backer, H., Jones, A. E., Bartlett, L., Vaughan, G., Goutail, F., Pommereau, J.-P., Kyro, E., Wahlstrom, C., Braathen, G., and Simon, P. C.: Validation of Ground-Based Visible Measurements of Total Ozone by Comparison with Dobson and Brewer Spectrophotometers, Journal of Atmospheric Chemistry, 29, 55–83, https://doi.org/10.1023/A:1005815902581, 1998.

Van Roozendael, M., Hendrick, F., Friedrich, M. M., Fayt, C., Bais, A., Beirle, S., Bösch, T., Navarro Comas, M., Friess, U., Karagkiozidis, D., Kreher, K., Merlaud, A., Pinardi, G., Piters, A., Prados-Roman, C., Puentedura, O., Reischmann, L., Richter, A., Tirpitz, J.-L., Wagner, T., Yela, M., and Ziegler, S.: Fiducial Reference Measurements for Air Quality Monitoring Using Ground-Based MAX-DOAS Instruments (FRM4DOAS), Remote Sensing, 16, 4523, https://doi.org/10.3390/rs16234523, 2024.

Vandaele, A. C., Hermans, C., Simon, P., Carleer, M., Colin, R., Fally, S., Mérienne, M. F., Jenouvrier, A., and Coquart, B.: Measurements of the NO2 absorption cross-section from 42 000 cm−1 to 10 000 cm−1 (238–1000 nm) at 220 K and 294 K, Journal of Quantitative Spectroscopy and Radiative Transfer, 59, 171–184, https://doi.org/10.1016/S0022-4073(97)00168-4, 1998.

Verhoelst, T., Compernolle, S., Pinardi, G., Lambert, J.-C., Eskes, H. J., Eichmann, K.-U., Fjæraa, A. M., Granville, J., Niemeijer, S., Cede, A., Tiefengraber, M., Hendrick, F., Pazmiño, A., Bais, A., Bazureau, A., Boersma, K. F., Bognar, K., Dehn, A., Donner, S., Elokhov, A., Gebetsberger, M., Goutail, F., Grutter de la Mora, M., Gruzdev, A., Gratsea, M., Hansen, G. H., Irie, H., Jepsen, N., Kanaya, Y., Karagkiozidis, D., Kivi, R., Kreher, K., Levelt, P. F., Liu, C., Müller, M., Navarro Comas, M., Piters, A. J. M., Pommereau, J.-P., Portafaix, T., Prados-Roman, C., Puentedura, O., Querel, R., Remmers, J., Richter, A., Rimmer, J., Rivera Cárdenas, C., Saavedra de Miguel, L., Sinyakov, V. P., Stremme, W., Strong, K., Van Roozendael, M., Veefkind, J. P., Wagner, T., Wittrock, F., Yela González, M., and Zehner, C.: Ground-based validation of the Copernicus Sentinel-5P TROPOMI \chemNO_2 measurements with the NDACC ZSL-DOAS, MAX-DOAS and Pandonia global networks, Atmospheric Measurement Techniques, 14, 481–510, https://doi.org/10.5194/amt-14-481-2021, 2021.

Weber, M., Arosio, C., Coldewey-Egbers, M., Fioletov, V. E., Frith, S. M., Wild, J. D., Tourpali, K., Burrows, J. P., and Loyola, D.: Global total ozone recovery trends attributed to ozone-depleting substance (ODS) changes derived from five merged ozone datasets, Atmospheric Chemistry and Physics, 22, 6843–6859, https://doi.org/10.5194/acp-22-6843-2022, 2022.

WMO: Scientific Assessment of Ozone Depletion: 2022, GAW Report No. 278, 509 pp, Geneva, 2022.

WMO: Sixteenth Intercomparison Campaign of the Regional Brewer Calibration Centre Europe, GAW report 301, 240 p., 2024.

https://doi.org/10.5194/egusphere-2025-5627
Preprint. Discussion started: 5 January 2026

Young, P. J., Naik, V., Fiore, A. M., Gaudel, A., Guo, J., Lin, M. Y., Neu, J. L., Parrish, D. D., Rieder, H. E., Schnell, J. L., Tilmes, S., Wild, O., Zhang, L., Ziemke, J., Brandt, J., Delcloo, A., Doherty, R. M., Geels, C., Hegglin, M. I., Hu, L., Im, U., Kumar, R., Luhar, A., Murray, L., Plummer, D., Rodriguez, J., Saiz-Lopez, A., Schultz, M. G., Woodhouse, M. T., and Zeng, G.: Tropospheric Ozone Assessment Report: Assessment of global-scale model performance for global and regional ozone distributions, variability, and trends, Elementa: Science of the Anthropocene, 6, 10, https://doi.org/10.1525/elementa.265, 2018.

Zerefos, C., Meleti, C., Balis, D., Tourpali, K., and Bais, A. F.: Quasi-biennial and longer-term changes in clear sky UV-B solar irradiance, Geophysical Research Letters, 25, 4345–4348, https://doi.org/10.1029/1998GL900160, 1998.

Zerefos, C. S., Meleti, C., Balis, D. S., Bais, A. F., and Gillotay, D.: On changes of spectral UV-B in the 90's in Europe, Advances in Space Research, 26, 1971–1978, https://doi.org/10.1016/S0273-1177(00)00167-8, 2000.

Zerefos, C. S., Balis, D. S., Zanis, P., Meleti, C., Bais, A. F., Tourpali, K., Melas, D., Ziomas, I., Galani, E., Kourtidis, K., Papayannis, A., and Gogosheva, Z.: Changes in surface UV solar irradiance and ozone over the balkans during the eclipse of August 11, 1999, Advances in Space Research, 27, 1955–1963, https://doi.org/10.1016/S0273-1177(01)00279-4, 2001.

Ziemke, J. R., Chandra, S., and Bhartia, P. K.: A 25-year data record of atmospheric ozone in the Pacific from Total Ozone Mapping Spectrometer (TOMS) cloud slicing: Implications for ozone trends in the stratosphere and troposphere, J. Geophys. Res., 110, 2004JD005687, https://doi.org/10.1029/2004JD005687, 2005.

Ziemke, J. R., Labow, G. J., Kramarova, N. A., McPeters, R. D., Bhartia, P. K., Oman, L. D., Frith, S. M., and Haffner, D. P.: A global ozone profile climatology for satellite retrieval algorithms based on Aura MLS measurements and the MERRA-2 GMI simulation, Atmos. Meas. Tech., 14, 6407–6418, https://doi.org/10.5194/amt-14-6407-2021, 2021.